A HYDROTHERMAL STUDY TO ESTIMATE VERTICAL GROUNDWATER FLOW IN THE CAÑUTILLO WELL FIELD, BETWEEN LAS CRUCES AND EL PASO

By
Shirley C. Wade
Graduate Research Assistant
New Mexico Bureau of Mines and Mineral Resources
and Geoscience Department
New Mexico Tech

and

Marshall Reiter
Principal Investigator
Senior Geophysicist,
New Mexico Bureau of Mines and Mineral Resources
Adjunct Professor of Geophysics, Geoscience Department
New Mexico Tech

TECHNICAL COMPLETION REPORT

Account Number 01345698

February 1994

New Mexico Water Resources Research Institute

in cooperation with

New Mexico Bureau of Mines and Mineral Resources
New Mexico Tech

The research on which this report is based was financed in part by the U.S. Department of the Interior, Geological Survey, through the New Mexico Water Resources Research Institute.

DISCLAIMER

The purpose of Water Resources Research Institute technical reports is to provide a timely outlet for research obtained on projects supported in whole or in part by the institute. Through these reports, we are promoting the free exchange of information and ideas, and hope to stimulate thoughtful discussion and actions that lead to resolution of water problems. The WRRI, through peer review of draft reports, attempts to substantiate the accuracy of information contained in its reports, but the views expressed are those of the author(s) and do not necessarily reflect those of the WRRI or its reviewers. Contents of this publication do not necessarily reflect the views and policies of the U.S. Department of the Interior, nor does mention of trade names or commercial products constitute their endorsement by the United States government.

ACKNOWLEDGMENTS

We are grateful for assistance provided to us by Scott Anderholm of the U.S. Geological Survey in Albuquerque, New Mexico and by Edward Nickerson of the USGS in Las Cruces, New Mexico. Edward Nickerson provided much useful information as well as hydrographs and well cuttings without which the project would not have been possible. We would also like to thank Roger Sperka with El Paso Water Utilities for the valuable detailed pumping information. Discussion with Fred Phillips of the New Mexico Tech Geoscience Department, provided insight into the possibility that remanent temperature distribution was present. Funding from the New Mexico Water Resources Research Institute and New Mexico Bureau of Mines and Mineral Resources made this study possible. Lynne Hemenway typed much of the report and Rebecca Titus drafted Figures 1 and 2.

ABSTRACT

The vertical component of specific discharge was estimated across several depth zones in the aquifer system at Cañutillo, Texas. The specific discharge was estimated with temperature and thermal conductivity data from four observation wells bottoming near the base of the aquifer system.

Specific discharge was first calculated (using a steady-state model) from slopes of conductive heat flow versus temperature. The heat-flow plots for all four wells suggested a zone of downward groundwater flow from ~70 to ~220 feet depth and one or two zones of upward flow from ~800 to ~220 feet depth. Head data from the observation wells supported the conclusion of an upper zone of downflow indicated by the temperature data; however, the head data suggested that groundwater should be currently moving downward from ~220 to ~800 feet.

We developed a computer model to determine if the temperatures may be remanent and therefore reflect prepumping groundwater flow, particularly in the deep flow zone. Estimates were made of both minimum original and during-pumping groundwater flow and maximum original and during-pumping flow. The computer model estimates and steady-state vertical specific discharge estimates were similar for the upper zone having downward flow. In the deep zone, specific discharge estimates modeled on the computer for minimum (prepumping) upflow agreed with steady-state heat-flow specific discharge estimates. Hence current temperature data may demonstrate a significant remanent groundwater flow component.

Key words: heat flow, temperature, groundwater, thermal conductivity, flow, aquifer

TABLE OF CONTENTS

LIST OF FIGURES

LIST OF TABLES

JUSTIFICATION OF WORK PERFORMED

The Cañutillo well field, located in Texas on the Texas-New Mexico border, between Las Cruces and El Paso, is an important source of water for the city of El Paso, Texas (Figure 1). The well field is underlain by an aquifer system comprised of four geologic zones; a shallow zone bottoming at ~80 feet depth, an upper intermediate zone from 80 feet down to about 250 feet depth, a lower intermediate zone from ~250 feet to 500 feet depth and a deep zone bottoming at about 900 feet depth (Nickerson 1989). We shall refer to an upper flow zone between 80 and ~220 feet depth and a deeper flow zone from ~220 to 800 feet depth (Figure 2).

The Rio Grande is connected hydraulically with the shallow zone (Nickerson 1989). The shallow zone is comprised of gravel and coarse- to medium-grained sand with thin discontinuous clay lenses. The upper intermediate zone contains alternating layers of fine- to coarse-grained sand, silty clay and gravel. The lower intermediate zone consists of medium- to fine-grained sand beds with a few silty clay lenses. The lower intermediate zone is separated from the deep zone by a continuous clay layer ranging in thickness from 20 feet at the western edge of the well field to 60 feet at the center of the well field (Figure 2). The deep aquifer contains uniform fine sand with some silt and clay. An impermeable limestone conglomerate lies below the deep zone (Nickerson 1986; 1989).

In 1985 four observation well nests were drilled in the Cañutillo well field to monitor water levels in the aquifer system underlying the well field. The piezometer nests consist of four wells, one bottoming in each geologic zone. The shallow piezometers are referred to as 1A-4A, the upper intermediate as 1B-4B, the lower intermediate as 1C-4C, and the deep as 1D-4D (Figure 2).

Temperature logs were taken in the deepest observation wells (1D-4D) by the U.S.

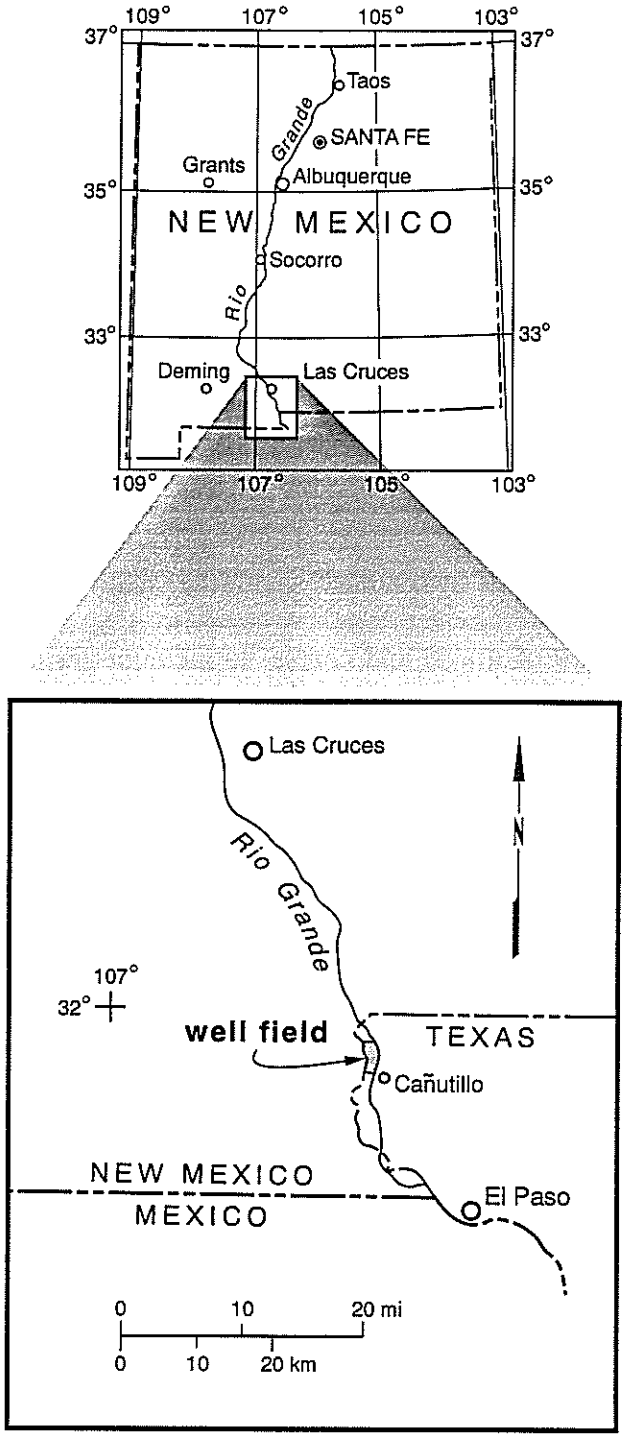

FIGURE 1. Study Area

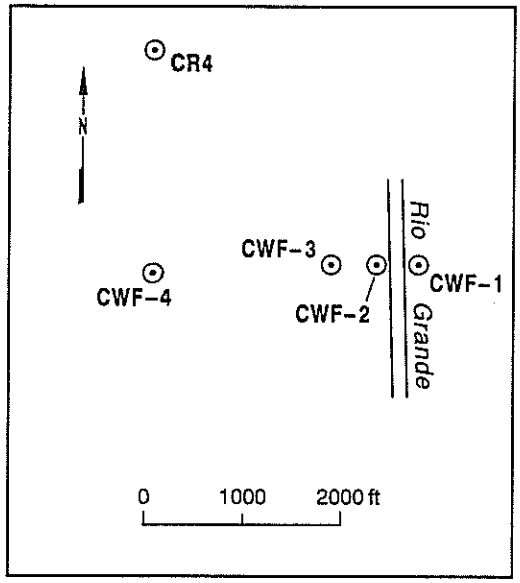

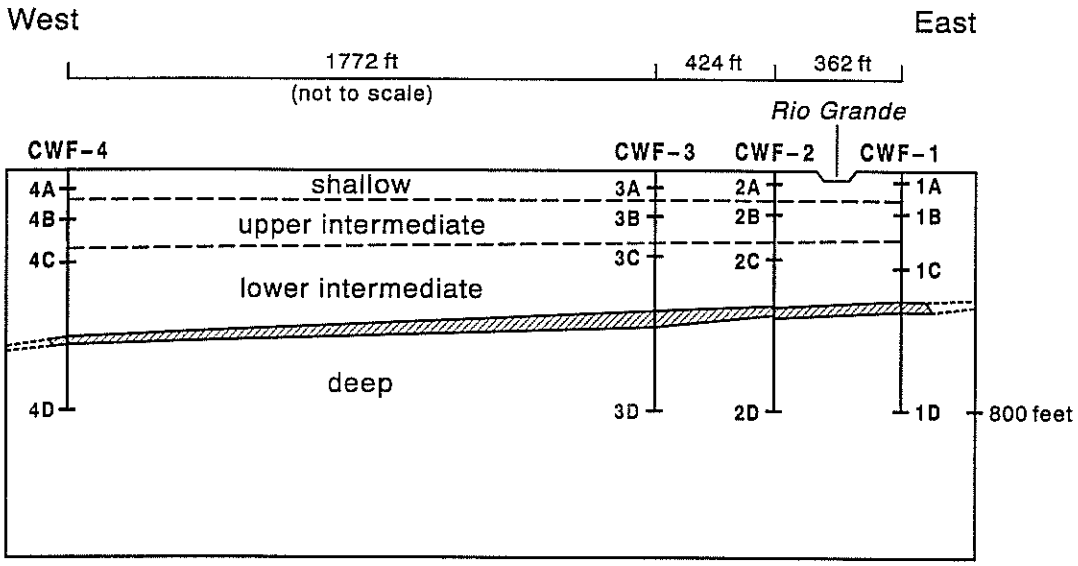

FIGURE 2. Study area and cross section. Each well nest represents four piezometers bottoming at A, B, C, and D. The temperature logs were taken in the deepest wells, D (after Nickerson 1989).

Geological Survey in December 1986 and February-March 1987 (Figure 3 shows digitized temperature logs made from the USGS temperature surveys). Temperature data in conjunction with thermal conductivity measurements can be used to estimate the specific discharge in an aquifer. Curved temperature profiles suggest either water movement or variation in rock thermal conductivities. Convex upward profiles suggest upward water flow or upwardly decreasing thermal conductivities; concave upward profiles suggest downward flows or downwardly decreasing thermal conductivities (Bredehoeft and Papadopulos 1965).

Under steady-state conditions a plot of conductive heat flow, Q, versus temperature, T, can be used to estimate vertical specific discharge. Since the vertical temperature gradient is typically orders of magnitude greater than the horizontal temperature gradient, the temperature profile is likely to be influenced mainly by vertical flow. Therefore the slope of the heat flow-temperature plot can be used to estimate the vertical component of water movement for the case where horizontal temperature gradients are negligible; where

$$\Delta Q = \rho c q_z (\Delta T) \tag{1}$$

and

Q = conductive heat flow

T = temperature

ρ = density of water

c = specific heat of water

q_z = vertical specific discharge

(Bredehoeft and Papadopulos 1965; Mansure and Reiter 1979; Reiter et al. 1989).

It initially appears that the temperature versus depth data may be somewhat inconsistent with the hydrographs taken in the observation wells. The four temperature

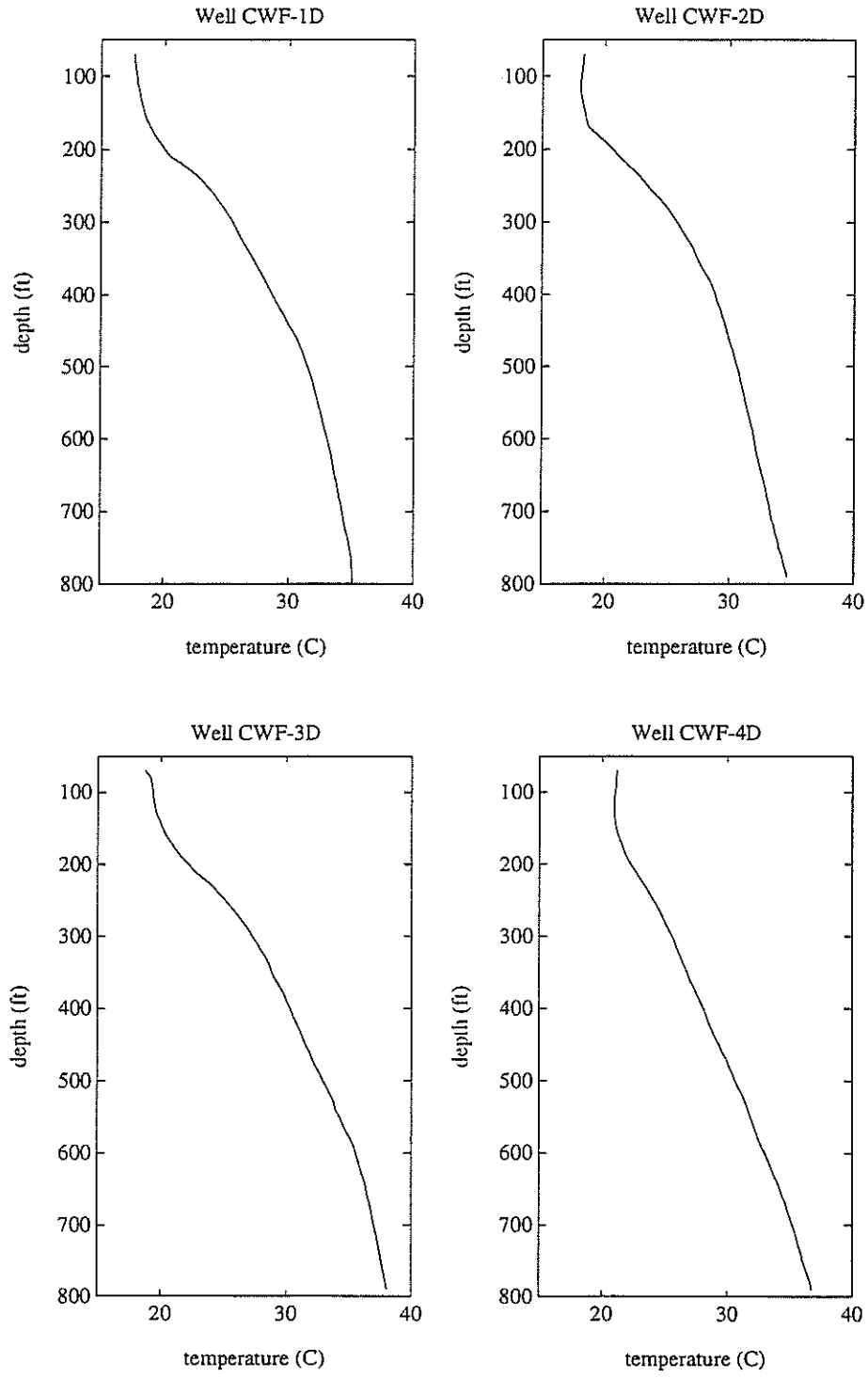

FIGURE 3. Temperatures measured in observation wells CWF–1D, CWF–2D, CWF–3D, and CWF–4D.

profiles from the Cañutillo well field are concave upward from the shallowest measurement depth to about 220 feet depth, and then become convex upward to about 800 feet depth. These curvatures suggest downward flow from 70 feet depth to about 220 feet depth and then upward flow from ~800 feet to ~220 feet depth. The hydrographs taken in the observation wells in 1986-1987 are consistent with the upper zone of downflow; however, they indicate downward flow from the intermediate to the deep zone (the water levels in the deep aquifer were below those in the intermediate zone over most of the 1987 water year; U.S.Geological Survey 1987). Two possibilities may explain this discrepancy: (1) variation of thermal conductivity is responsible for the curvature in the temperature data; (2) the temperature data are the net effect of present and past flow. These possibilities are discussed in the following sections.

METHODOLOGY

Thermal Conductivity Measurements

Because curvature in temperature profiles over the depth of a well can be caused by both water movement and variations in thermal conductivity, it is important to measure thermal conductivity over the depth of the observation well. Well cuttings were available from the four deep observation wells in the Cañutillo well field (Figure 2). The thermal conductivities of the aquifer material were measured at New Mexico Tech's thermal conductivity laboratory. The method of measurement is described in Reiter and Hartman (1971) and Sass et al. (1971).

The aquifer material (sand, gravel and/or clay) was packed into small disk-like cells 1.5 inches in diameter and about 0.5 inch in height. The cells were vacuum flooded with distilled water and then placed under about 200 psi pressure between an ohmic heater and a

massive aluminum block. A known amount of heat was applied to the top of the cell and the temperature drop across the cell was measured with a pair of thermocouples. By knowing the heat flux into the top of the cell, the temperature drop across the cell, and the geometry of the cell, the conductivity for the aggregate material in the cell was calculated. Known standards were used for comparison.

A geometric model was used to convert from the conductivity of the aggregate in the cell to the conductivity of the rock matrix (Sass et al. 1971; Beck 1976). A porosity correction was then necessary to calculate the in situ rock conductivity from the laboratory-measured rock matrix conductivity. The aquifer material's porosities were estimated from neutron geophysical logs taken in the four observation wells. The logs were scaled according to a neutron log taken elsewhere by the same logging operator with probably the same equipment and the scale extrapolated to the counts per second on the Cañutillo well logs. As a result, there is some uncertainty associated with the absolute porosities. However, the porosities appear to vary relatively little over the depth of the well, which is valuable qualitative information used to support the importance of the temperature logs. The aquifer conductivities were estimated from the aquifer porosity and the rock matrix conductivity. The thermal conductivities, porosities, temperature gradients, and calculated conductive heat-flow values are listed for wells CWF-1D - CWF-4D in Appendix C, Tables 13-16.

Even though uphole sloughing is likely to occur during sample gathering, the large temperature gradient changes over the study wells should be accompanied by noticeable thermal conductivity changes if groundwater flow is absent; such conductivity change was not measured. In addition, six samples over the depth of one of the wells were further washed in the lab to remove any remaining drilling mud. Conductivity values for these washed samples, compared to values for unwashed samples from the same depth intervals,

showed no untypical variation. Therefore, we assume that the samples are relatively free of drilling mud.

TEMPERATURE DATA AND HEAT FLOW—STEADY-STATE MODEL

The original temperature logs were digitized at ten-foot intervals. The temperature gradients were then calculated at twenty-foot intervals to correspond to the thermal conductivity measurements made over twenty-foot intervals. The digitized temperature profiles are shown in Figure 3. The thermal conductivity, K, and the temperature gradient, dT/dz, were used to calculate the conductive heat flow, Q, over each of the twenty-foot intervals, where

$$Q = -K(dT/dz) \tag{2}$$

(Currie 1974). Plots of conductive heat flow versus temperature are shown in Figure 4. If the temperatures are steady-state, the slope of the conductive heat-flow plots can be used to calculate the vertical component of specific discharge with Equation 1.

The wells were divided into several zones based on the heat flow versus temperature plots and a vertical component of flow was calculated for each zone. If the heat flow-temperature graph clearly changed slope a new flow zone was assumed. The flow zone boundaries roughly coincided with hydrogeologic boundaries in most cases. However, results presented here seem to suggest that the boundary between the upper and lower intermediate aquifers may lie at a depth shallower than the 250 feet depth previously suggested (Figure 4; slope change occurs at temperatures corresponding to depths shallower than 250 feet). The heat flow-temperature plots for all four wells indicated downflow from the upper intermediate to the lower intermediate zone and generally upflow from the deep to the lower

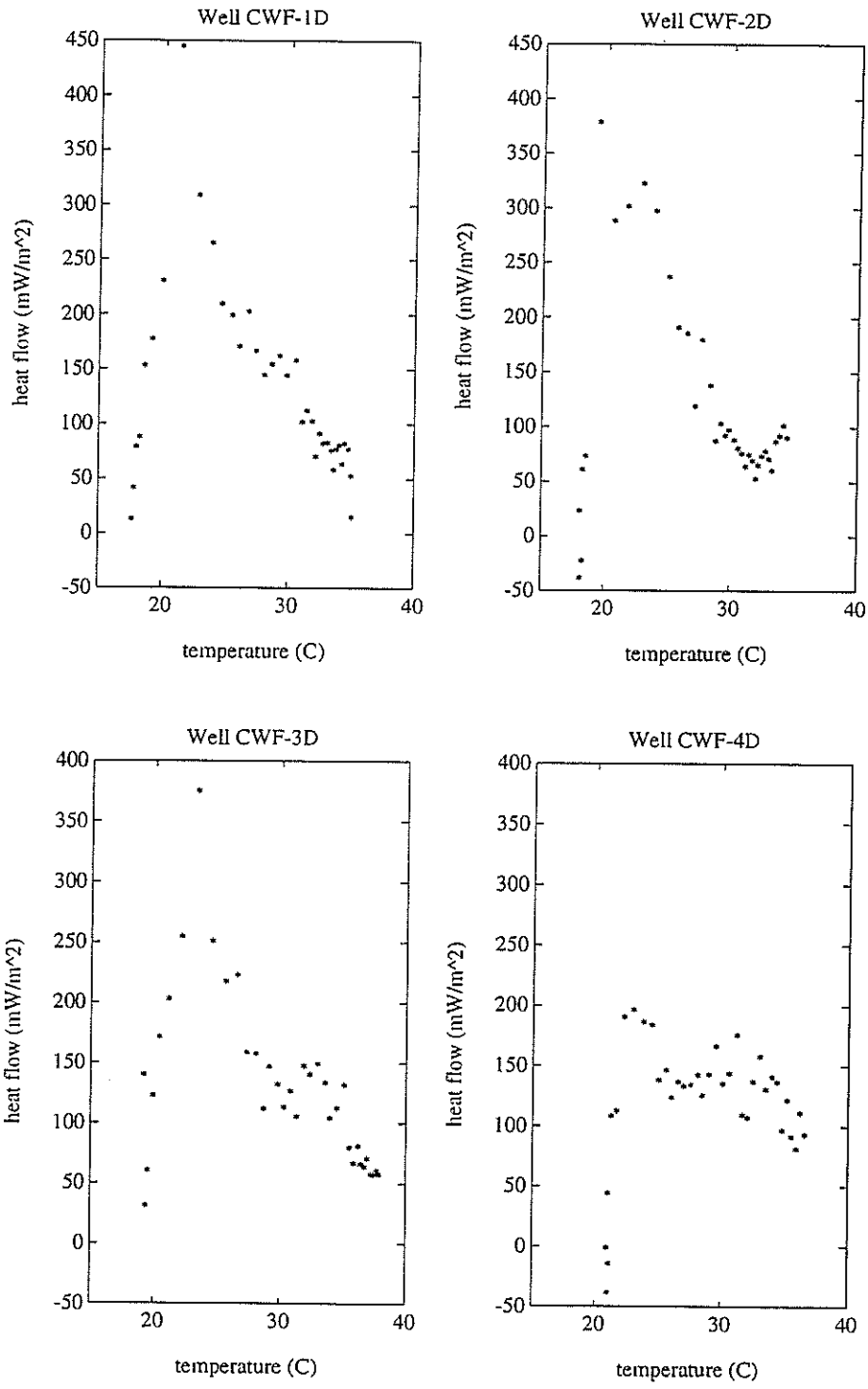

FIGURE 4. Heat flow ($-k\Delta T/\Delta z$) versus temperature, calculated from measured thermal conductivities and temperatures.

intermediate zone (Figure 2). In this report the upper flow zone corresponds to flow through the upper intermediate (aquifer) zone to the top of the lower intermediate aquifer and the deep flow zone corresponds to flow from the lower intermediate to the deep (aquifer) zone. Flow in the shallow (aquifer) zone, above ~70 feet, could not be estimated because temperature data were unavailable above 70 feet.

Well CWF-1D was divided into two flow zones. An upper zone of downflow to 230 feet (22.1°C) was suggested by the temperature log as well as the Q (heat flow) versus T (temperature) plot (Figures 3 and 4). A deeper zone, apparently upflowing, from 800 feet (35.15°C) to about 230 feet (22.1°C) is also suggested by both the temperature log and the Q-T plot (Figures 3 and 4). The flow rates (determined by a least squares fit of Q versus T) are listed in Table 1 along with the correlation coefficients. The mismatch of the Q-T plot at the top of the deep zone (Figure 4), implies a condition not appropriate for our model, such as transient temperatures or horizontal temperature gradients. The points representing depths of 240 feet (22.8°C) and 260 feet (23.85°C) were disregarded and the flow recalculated excluding these points (Table 1, little difference in the upflow rates was noticed).

Well CWF-2D was divided into three flow zones based on the heat flow versus temperature plots; an upper zone with downflow from 110 to 170 feet depth (18.05°C to 18.7°C), a deeper zone of apparent upflow from 600 to 190 feet (32.0°C to 20.0°C), and a deep zone with apparent downflow from 600 to 790 feet (32.0°C to 34.65°C). Heat flow values at 80 and 100 feet depth (18.25°C and 18.1°C) were disregarded because the temperature gradients were negative and vertical flow cannot produce negative temperature gradients in our model. Negative temperature gradients can be caused by horizontal ground-water flow in the presence of horizontal temperature gradients or by long-term climate change. The flow rates are listed in Table 1.

TABLE 1. Vertical specific discharge calculated from the slope of the heat flow-temperature plots.

Well	Zone (depth in feet)	Vertical specific discharge (cm/sec)	r
1D	70-230	2.6×10^{-6}	0.98
1D	230-800	-4.2×10^{-7}	-0.96
1D	270-800	-3.7×10^{-7}	-0.95
2D	110-170	2.6×10^{-6}	0.98
2D	190-600	-6.0×10^{-7}	-0.96
2D	600-790	3.7×10^{-7}	0.84
3D	70-230	1.7×10^{-6}	0.94
3D	230-790	-2.8×10^{-7}	-0.90
4D	110-220	2.1×10^{-6}	0.91
4D	220-280	-6.1×10^{-7}	-0.85
4D	280-510	4.5×10^{-8}	0.31
4D	510-790	-2.3×10^{-7}	-0.63
4D	220-790	-1.1×10^{-7}	-0.69

*Note: r = correlation coefficient

Using heat flow-temperature plots Well CWF-3D was divided into two flow zones; an upper zone of downward water flow from 70 to 230 feet depth (18.75°C to 24.09°C) and a deeper zone of apparent upward groundwater flow from 790 to 230 feet depth (38°C to 24.09°C). Again, flow rates are listed in Table 1.

We initially divided well CWF-4D into two flow zones; an upper zone with downflow from 110 to 220 feet depth (20.95°C to 23.0°C), and a deeper zone of apparent upflow from 790 to 220 feet (36.7°C to 23.0°C). After closer inspection of the heat flow-temperature data for Well-4D we also suggested four groundwater flow zones; an upper flow zone with downflow from 110 to 220 feet depth (20.95°C to 23.0°C), a deeper zone of apparent upflow from 280 to 220 feet (25.0°C to 23.0°C), a zone of apparent downflow from 280 to 510 feet (25.0°C to 30.9°C), and a zone of upflow from 790 to 510 feet (36.7°C to 30.9°C) (Table 1). As with Well CWF-2D, the two heat flow values for Well CWF-4D at depths 80 and 100 feet (21.1°C and 21.0°C) were disregarded because the temperature gradients were negative. It should be noted that a change in vertical groundwater flow from one zone to another must be accompanied by an equivalent change in horizontal groundwater flow.

TRANSIENT MODEL

The vertical specific discharge values calculated from the slopes of the heat flow versus temperature plots were based on an assumption of steady-state aquifer temperatures and steady-state groundwater flow. However, hydrologic conditions have changed considerably in recent decades at this location. After pumping of the deep and intermediate aquifers began in the late 1950s, the head gradient across the confining clay layer between the lower intermediate and deep aquifers was reversed from upward to downward. Water

levels in the first production wells drilled in the deep aquifer were nine feet above water levels in the lower intermediate aquifer. After 1956 water levels in the deep aquifer were usually at least ten feet below water levels in the lower intermediate aquifer (El Paso Water Utilities, 1992). This head gradient reversal would have reversed the direction of vertical groundwater flow from upward to mostly downward. The impact of this downward water flow on the temperatures in the lower intermediate and deep aquifers was evaluated in the present study using a transient one-dimensional finite-difference advection-diffusion model.

Water levels from 1956 to 1986 in the upper and lower intermediate aquifers were consistent with downward groundwater flow to about 220 feet depth; therefore, our estimates of downward groundwater flow in the upper zones (above ~220 feet) from a steady-state model are probably reasonable. There has, however, been a decrease in the water level in the lower intermediate zone as a result of pumping, therefore the upper flow zone was also modeled with an increase in downward flow after 1956.

The one-dimensional advection-diffusion equation is given by

$$\frac{\partial T}{\partial t} = \frac{-C_w \rho_w}{C_s \rho_s} q_z \frac{\partial T}{\partial z} + \frac{K}{C_s \rho_s} \frac{\partial^2 T}{\partial z^2} \qquad (3)$$

where

T = temperature (degrees C)

t = time (seconds)

C_w = specific heat of water

ρ_w = density of water

q_z = vertical specific discharge of water

z = depth

K = thermal conductivity of aquifer

C_s = specific heat of aquifer

ρ_s = density of bulk saturated aquifer material

(Stallman 1963).

The assumptions for this partial differential equation are: (1) K, C, and ρ are constant, (2) horizontal temperature gradients are negligible, (3) water is incompressible, and (4) viscous effects are negligible. Typically horizontal temperature gradients are small when compared with vertical temperature gradients. For a more complete understanding of horizontal gradients in this study one would need temperature data at a number of sites, some located outside the well field. The fact that shallow temperatures are cooler near the river (sites 1D and 2D, Figure 3) is consistent with vertical flow from the river influencing subsurface temperatures more at sites closer to the river. It seems unlikely that horizontal flow would cool sites at the river and warm sites away from the river. The shallow horizontal temperature gradient is greatly reduced away from the river (compare temperatures at sites 3 and 4 to those at sites 2 and 3), suggesting any horizontal flow will be of lesser influence away from the river (even though all the temperature logs appear curved). The pumping of the well field also surely affects the horizontal flow. At present, the most straightforward explanation for the curvature in the temperature logs is vertical flow.

A finite-difference approximation to the differential equation was made using an approximation to the advection-dispersion equation for solute transport given in Bear and Verruijt (1987). The finite-difference equation is given by

$$T\,(z,\ t+dt)\ -\ T\,(z,t)\ =\ \frac{-C_w\rho_w}{C_s\rho_s}\ q_z\ \frac{[T\,(z\ +\ dz,t)\ -\ T\,(z\ -\ dz,t)]}{2dz}\ +$$

$$\frac{K}{C_s\rho_s}\left[\frac{T\,(z\,+\,dz,t)\,-\,2T\,(z,t)\,+\,T\,(z\,-\,dz,t)}{dz^2}\right]. \qquad (4)$$

A FORTRAN computer program was written to solve Equation 4 at time step t_o + dt given $T(z,t_o)$. The difference equation is stable provided the following conditions are met (Bear and Verruijt 1987):

$$dt \leq \frac{1}{2}\,(dz)^2\,\frac{C_s\rho_s}{K} \qquad (5)$$

and

$$q_Z \leq \frac{dz}{dt}\left(\frac{C_s\rho_s}{C_w\rho_w}\right). \qquad (6)$$

.

With the depth interval in our case equal to 10 feet, dz = 304.8 cm (10 feet), $C_s\rho_s/K$ = 226.8 sec/cm^2, and $C_s\rho_s/C_w\rho_w$ = 0.91 (Keys and Brown 1978). Therefore the time interval should be such that dt $<$ 1.05 x 10^7 seconds for computational stability. If dt = 1.0 x 10^6 seconds (as we choose) then, q_z $<$ 2.77 x 10^{-4} cm/sec (from the above equations). For all solutions the time increment was 1.0 x 10^6 seconds and the maximum velocity in any of the solutions was 8.8 x 10^{-6} cm/sec; as such the stability criteria were met in all cases. The thermal conductivity, K, was assumed to be constant and equal to 4.0 mcal/cm-sec-°C (roughly the average measured thermal conductivity; Appendix C, Tables 13-16). The FORTRAN program is presented in Appendix A. Input variables in the program were the number of time steps and the vertical specific discharge (negative upward or positive

downward). Verification of the computer model using analytical solutions is detailed in Appendix B.

Modeling the data

The temperature profiles for the four wells in our study were divided into two major zones, an upper portion suggesting downward groundwater flow from 70 feet depth to about 220 feet depth and a deeper portion suggesting upward groundwater from the bottom of the wells to about 220 feet depth. Several models were developed for each flow zone using the transient numerical solution presented above (Equation 4) with the top and bottom temperatures of each flow zone held constant through time. The calculated temperatures were then compared to the measured temperatures for each numerical model. The sum of the squares; $ss = \Sigma (tm\text{-}td)^2$, where tm is the measured temperature and td is the calculated temperature, was used as a quantitative measure of how well the numerical model described the observed data. Best fit temperature curves were pursued by varying flow rates in the model (prepumping flow rates in some cases and during-pumping flow rates in other cases) until the sum of squares reached a minimum value.

Head data from the upper zone suggest continued downflow both prior to and after 1956. This upper concave portion of the data was compared to three models; (1) a steady-state temperature curve resulting from constant downward flow for about 1200 years, (2) a temperature curve resulting from no water flow before 1956 and significant downward flow from 1956 to 1986, and (3) a temperature curve caused by some smaller initial downward flow before 1956 and an increased flow beginning in 1956 when pumping began in the intermediate aquifer (Table 2). The steady-state temperature curve for the first case was established by determining what downward flow produced temperatures that best fit the

TABLE 2. Computer model case descriptions for flow in the upper flow zone and in the deep flow zone.

Case	Description
	Upper Flow Zone
1	a steady-state temperature profile resulting from constant downward flow for ~1200 years
2	a temperature profile resulting from no water flow before 1956 and significant downward flow from 1956 to 1986
3	a temperature profile caused by an initial downward flow (see text) before 1956 and an increased flow beginning in 1956
	Deep Flow Zone
1	a minimum prepumping upward discharge was estimated by assuming no downward flow for 30 years
2	a maximum prepumping upward flow was estimated by assuming maximum downflow for 30 years over most of the flow zone (excluding the top 100 feet, ~200-~300 feet depth, where no vertical flow seems to have occurred)
3	an initial upward flow was estimated by assuming downflow between about 300 and 800 feet depth which was calculated from pumping information for 1956 to 1986 (again no vertical flow from ~200 to ~300 feet depth)

measured data after ~1200 years. The significant downward flow for the second case was established by using a linear temperature gradient as initial conditions in the model and determining what downward flow over 30 years produced a curve that best fit the measured data. An initial downward flow for the third case was estimated from a water level measured in the upper intermediate aquifer and a water level measured in the lower intermediate aquifers when the first production wells in those aquifers were drilled. (These wells were not at the same horizontal location so the initial flow is a first order estimate.) The final downflow in the third case, from 1956 to 1986, was that vertical specific discharge which provided modeled temperatures that best fit the data.

To assess the effect 30 years of downward groundwater flow in the deep flow zone (the lower intermediate and deep aquifers) has had on the temperature profile, an initial established profile had to be estimated. This profile was calculated using the finite-difference equation with upward flow. A linear temperature gradient calculated from the temperatures at the top and bottom of the zone of interest was used as an initial condition in the model. It is therefore assumed that the temperatures at the top and bottom of the zone of interest have not changed over time. Upward flow was modeled for 1268 years, a length of time determined to be sufficient for the initial temperature profile to be steady-state (temperatures after 2536 years were not significantly different from those after 1268 years.)

The prepumping upflow in the deep flow zone (between the intermediate and deep aquifers) was estimated for three cases by making assumptions about downflow during the thirty years of pumping (1956-1986). The prepumping upflows for these three cases were established so that the initial, 1956, temperature profile would ultimately yield a best fit to the measured temperatures after 30 years of subsequent downflow. The three cases were: (1) an initial minimum upflow was estimated by assuming no downward flow for 30 years, (2) a

maximum prepumping upward flow was estimated by assuming maximum downflow for 30 years over most of the flow zone (excluding the top 100 feet where no vertical flow is assumed to have occurred), and (3) a prepumping upward flow was estimated by assuming a downflow between about 300 and 800 feet depth calculated from pumping information for 1956 to 1986 (again no vertical flow from ~200 to ~300 feet depth, Table 2). The maximum downward discharge across the clay layer in Case 2 (Figure 2) was determined by assuming the maximum head difference observed in 1986-1987 ocurred across the clay layer only. The hydraulic conductivities for the hydrogeologic units have been estimated to be 0.00917 cm/sec (26 ft/day) in the upper and intermediate aquifers, 0.00388 cm/sec (11 ft/day) in the deep aquifer and 3.5×10^{-6} cm/sec (0.01 ft/day) in the clay layer (Nickerson 1989). The computer model case descriptions for the upper flow zone and the deep flow zone are summarized in Table 2.

Checking the transient model at large times

The final temperature distribution after 1268 years (just prior to pumping) should depend only on the groundwater flow rate and the boundary temperatures. The sensitivity of the finite-difference solutions to initial (t = 0) temperature profiles was evaluated by applying the same upward flow for 1268 years (40 billion seconds) to both the measured temperature data and to temperatures calculated along a linear gradient keeping the top and bottom temperatures fixed as measured. The resulting temperature profiles were the same, that is, the sum of the squares of the difference between the two resulting profiles was zero. Therefore, the computer model is not sensitive to reasonably different initial temperature profiles for long time solutions, as should be the case.

PUMPING SCHEDULES

Pumping schedules available for the years 1956 through 1991 (El Paso Water Utilities 1992) made it possible to estimate the average vertical component of specific discharge for the period 1956 to 1986 in the upper and lower flow zones. The average vertical flow from the upper to lower intermediate aquifers was then compared to the downflow rates estimated with the computer model for downflow in the upper flow zone. The average vertical specific discharges estimated from the pumping schedules for flow from the lower intermediate to the deep aquifer (deep flow) were used as one estimate of during-pumping downflow in the computer model (Case 3 deep flow zone; Table 2).

Yearly pumping volumes (gallons) were listed for each production well in the Cañutillo well field. In addition, the pumping schedules included monthly pumping rates and volumes for 1971 through 1992 (El Paso Water Utilities 1992).

Correlation of monthly pumping to heads in 1986-1991

Water level data in the observation wells were available from 1986 to 1991 (the observation wells were drilled in 1984-85). However, to estimate the head data prior to 1986 and after 1956 in the lower intermediate and deep aquifers, we had to derive a correlation between the water level in the observation wells and the total average pumping rate in the lower intermediate and deep aquifers from 1986 to 1991. The total average pumping rate was the sum of monthly average pumping rates for all production wells in an aquifer. The water levels were plotted against the total average pumping rate in gallons/minute for the month in which the water level measurement was taken. We then applied this correlation to the 30 year (1956-1986) total average pumping rate, derived from yearly pumping volumes, and estimated the heads.

The water level in the upper intermediate aquifer appeared much less dependent on pumpage than did the levels in the lower intermediate and deep aquifers. Therefore, the water levels in wells 1B-4B (upper intermediate piezometers; Figure 2) were correlated with equivalent water levels in another close observation well (CR4) for which measurements were available during the entire 30 years of pumping. Therefore, for the upper intermediate aquifer, we did not have to correlate water levels to total average pumping rate. Between 1986 and 1992, the water levels in observation well CR4, located 2400 feet north of well group CWF-4 (Figure 2), were correlated with the upper intermediate water levels in each of wells CWF-1B, 2B, 3B, and 4B. A least squares fit was made to the head versus head values and the slope, y-intercept, and correlation coefficient were calculated. These parameters were then used to estimate the water levels in the four upper-intermediate aquifer observation wells (1B-4B) in the period 1956-1986. The line fitting parameters are listed in Table 3 as well as the estimated average heads.

Correlations were made between head and total average pumping rate in the lower intermediate and deep aquifer. The water level and the date measured were noted and the monthly average pumping rate in each production well in that aquifer was recorded (water levels were measured about twice a year, so there were about two points on the head-pumping graph per year). A linear least squares fit was made to the head versus total average pumping rate (sum of all average pumping rates). The case that provided the best correlation was choosen for estimating the yearly water levels for 1956 to 1986.

There are six production wells that are screened in the deep aquifer and nine production wells screened in the intermediate aquifer. Correlations between deep production and hydraulic head in the deep aquifer were made for two cases: (1) all six deep production wells and (2) for only the three closest deep production wells. The water levels in the four

TABLE 3. Correlation parameters and estimated average heads below ground surface for 1956 to 1986.

Well	A (ft)	B	r	P	CR4 average head (ft)	Total average pumping rate (gal/min)	Estimated average head[1,5] (ft)
1B	8.4	1.097	0.71	0.01	11.45	—	20.96
2B	0.63	1.28	0.79	0.01	11.45	—	15.29
3B	2.69	1.07	0.55	0.1	11.45	—	14.94
4B	3.14	0.58	0.76	0.01	11.45	—	9.78
1C	15.91	0.00936	0.69	0.01	—	1760[2]	32.38
2C	12.11	0.00980	0.69	0.01	—	1760	29.37
3C	11.15	0.0106	0.70	0.01	—	1760	29.81
4C	4.92	0.0052	0.54	0.05	—	3350[3]	22.34
1D	31.38	0.00427	0.70	0.01	—	5796[4]	56.13
2D	30.01	0.00412	0.67	0.01	—	5796	53.89
3D	36.24	0.00374	0.48	0.1	—	5796	57.92
4D	26.29	0.0036	0.63	0.02	—	5796	47.16

*note:
A = y-intercept
B = regression coefficient
r = correlation coefficient
P = probability that heads are not correlated

1. Calculated using linear least mean squares fit parametrs and average head from CR4 or average pumping rate.
2. Correlation best for total average pumping rate calculated for four nearby wells.
3. Correlation best for total average pumping rate calculated for nine wells in field.
4. Correlation best for average total pumping rate calculated for all six wells in field.
5. Heads indicate depth below the ground surface.

deep observation wells, 1D-4D, were best correlated with pumpage in all production wells screened in the deep aquifer. Similarly, in the intermediate aquifer the correlation between intermediate depth production and hydraulic head (in observation wells 1C-4C) was made for all nine production wells, and for only the four nearest production wells. With the exception of observation well CWF-4C, it was determined that the correlation based only on the four closest production wells in the intermediate aquifer achieved the best fit between production and head values in the observation wells. The correlation based on all intermediate pumping wells produced the best fit in Well 4C. The correlation parameters and estimated average heads are listed in Table 3.

Estimation of average vertical discharge from 1956-1986 using head correlations

The average yearly pumpage (gallons) for the 30-year period in the lower intermediate and deep zones were converted to average pumping rates in gallons per minute. The pumping rates were multiplied by the regression coefficient, B, and added to the intercept to produce the estimated average heads for 1956-1986 listed in Table 3. Several of the total average pumping rates for the intermediate and deep aquifers lay outside of the range of pumping rates used to establish the correlation parameters; therefore, water levels based on these outlying pumping rates were extrapolated rather than interpolated.

The estimated vertical specific discharge was calculated with Darcy's law,

$$q_z = K_h \frac{\Delta h}{\Delta l} \tag{7}$$

where

q_z = vertical specific discharge

K_h = vertical hydraulic conductivity

dh/dl = vertical hydraulic gradient between observation wells C and D screened in the intermediate and deep aquifers, respectively.

The effective hydraulic conductivity for a system of rock layers where water flow is perpendicular to the layers is given by

$$K_h = \frac{\sum L_i}{\sum \frac{L_i}{K_i}} \tag{8}$$

where

L_i = thickness of the ith layer

K_i = vertical hydraulic conductivity of the ith layer

(Freeze and Cherry 1979).

The hydraulic conductivities used to calculate the effective vertical hydraulic conductivities are those given by Nickerson (1989) for the aquifer and confining clay layer. The hydraulic conductivities, the head gradients and the estimated average vertical component of specific discharge from the upper intermediate to the lower intermediate aquifer and from the lower intermediate to the deep zone are listed in Table 4. The hydraulic heads in the deep aquifer were not adjusted downward for density contrast due to higher temperatures. The maximum correction for decreased density would have been about one and a half feet which is at least an order of magnitude less than the observed head differences and within the uncertainty of the estimated heads.

While we recognize that the pumpage-water level relationships show poor correlation, particularly for low values of pumpage, this seemed the only method of estimating head

TABLE 4. Average gradients and vertical specific discharge for 1956 to 1986 estimated using head data from upper intermediate and lower intermedite aquifers and from lower intermediate and deep aquifers (Figure 2).

Wells	Keff (cm/sec)	$\Delta h/\Delta l$	Vertical specific discharge (cm/sec)	Correlation
		Upper Flow Zone		
1B - 1C	5.6×10^{-5}	0.064	3.6×10^{-6}	e-e
2B - 2C	5.6×10^{-5}	0.099	5.6×10^{-6}	e-e
3B - 3C	5.6×10^{-5}	0.106	6.0×10^{-6}	i-e
4B - 4C	5.6×10^{-5}	0.090	5.1×10^{-6}	i-e
		Deep Flow Zone		
1C - 1D	3.28×10^{-5}	0.051	1.7×10^{-6}	e-i
2C - 2D	2.33×10^{-5}	0.049	1.1×10^{-6}	e-i
3C - 3D	1.41×10^{-5}	0.056	7.9×10^{-7}	e-i
4C - 4D	3.49×10^{-5}	0.050	1.7×10^{-6}	e-i

*note:

Keff = effective vertical hydraulic conductivity. Because vertical hydraulic conductivity values are not explicitly available for the aquifer sections, we used the given aquifer hydraulic conductivity for the aquifer and the vertical hydraulic conductivity for the clay layers (as given in Nickerson 1989). Hopefully the difference between K_{vert} and K_{horiz} is not too large in the aquifer; at any rate this is the best one can do with available data, and in addition, the use of Equation 8 biases the conductivity estimate toward the low values estimated for K_{vert} in clay.

correlation -- e = water level in well was extrapolated
-- i = water level in well was interpolated

gradients at the same map location as the temperature gradients were measured. Historical miscellaneous water levels would give vertical head gradients for a different location in the well field (in the case where water levels were from two different depths at the same map location) or would give head gradients with some unknown component of horizontal head gradient (in the case of water levels measured at two different map locations. Any of these three methods gives an estimated vertical head gradient with a large degree of uncertainty.

DISCUSSION OF RESULTS

COMPUTER MODEL RESULTS

Upper flow zone (upper intermediate to lower intermediate aquifer)

The results of the three cases presented above to investigate the concave upward portion of the temperature data, are summarized in Table 5. The sum of the squares of the differences between calculated and measured temperatures are also listed. The steady-state downward flows in Case 1 (i.e., the same flow before and after pumping; Table 2) that produced temperatures which best fit the data were 2.3×10^{-6} cm/sec, 1.9×10^{-6} cm/sec, 1.6×10^{-6} cm/sec, and 2.4×10^{-6} cm/sec for wells CWF-1D, -2D, -3D, and -4D, respectively. The final temperature curves are shown with the measured temperature data in Figure 5.

The downflows in the upper zone determined from Case 2 (no prepumping flow and maximum downflow from 1956 to 1986), ranged from 1.7×10^{-6} cm/sec at well 3D to 2.5×10^{-6} cm/sec at well 1D. Calculated temperature curves for Case 2 are shown along with the estimated initial temperatures and the measure data in Figure 6. The flow rates for Case 3 (based on an initially established flow rate of about 4.0×10^{-7} cm/sec downward prior to 1956) were between 1.7×10^{-6} and 2.5×10^{-6} cm/sec downward for the 30-year period 1956

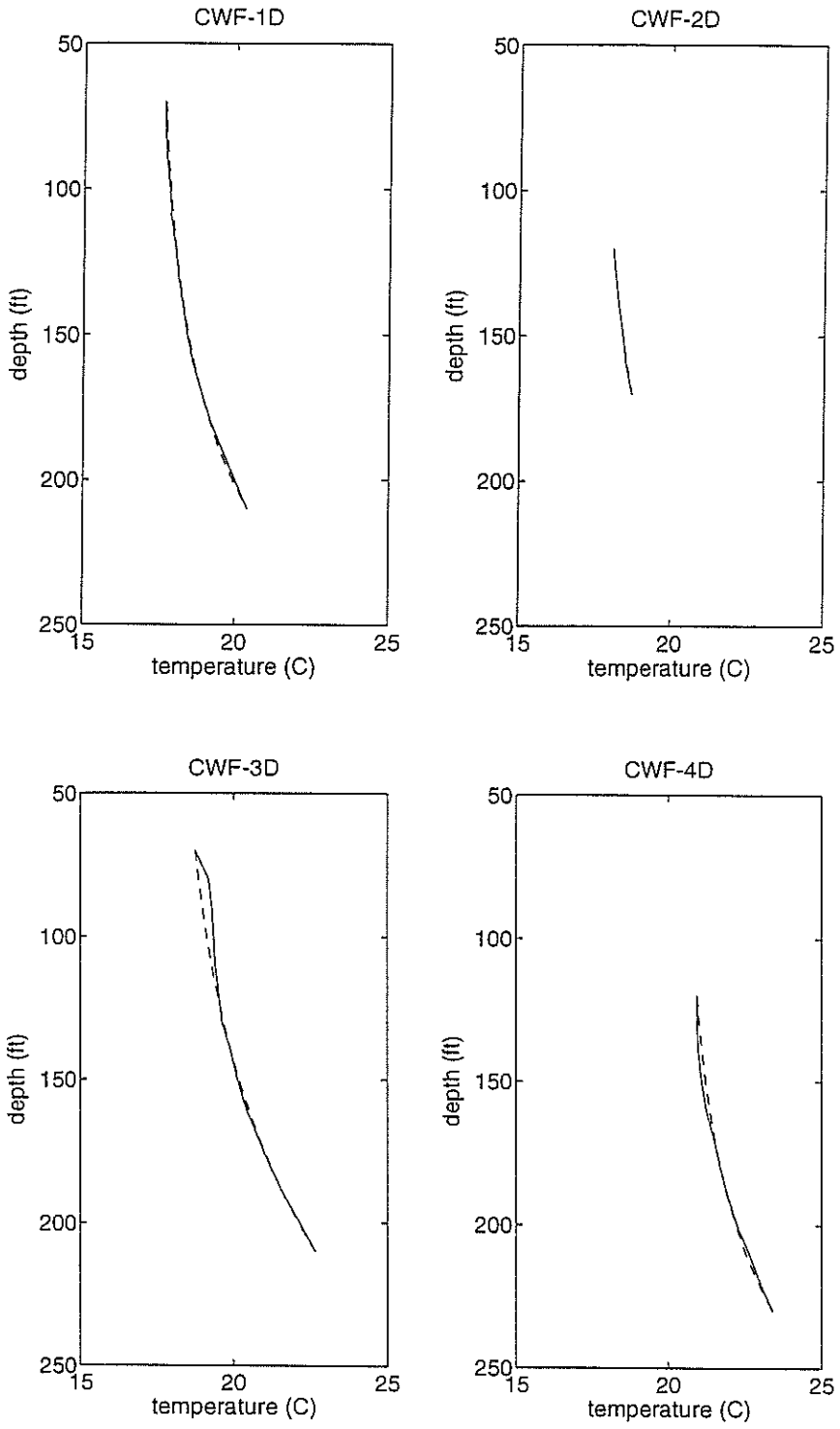

FIGURE 5. Upper flow zone, Case 1 (same vertical flow before and after pumping began; see text).
——— measured temperatures
- - - - - - - calculated 1986 temperatures

TABLE 5. Results for three upper flow zone cases.

Case	Well	Zone (depth, feet)	qo (cm/sec)	q (cm/sec)	Sum of squares $\Sigma (Tm - Tc)^2$
1	1D	70-210	2.3×10^{-6}	2.3×10^{-6}	0.03
1	2D	120-210	1.9×10^{-6}	1.9×10^{-6}	0.001
1	3D	70-210	1.6×10^{-6}	1.6×10^{-6}	0.287
1	4D	120-230	2.4×10^{-6}	2.4×10^{-6}	0.07
2	1D	70-210	0.0	2.5×10^{-6}	0.04
2	2D	120-170	0.0	2.0×10^{-6}	0.001
2	3D	70-210	0.0	1.7×10^{-6}	0.283
2	4D	120-230	0.0	2.5×10^{-6}	0.07
3	1D	70-210	4.0×10^{-7}	2.5×10^{-6}	0.04
3	2D	120-170	4.0×10^{-7}	1.9×10^{-6}	0.001
3	3D	70-210	3.5×10^{-7}	1.7×10^{-6}	0.284
3	4D	120-230	4.0×10^{-7}	2.4×10^{-6}	0.07

*note:

Case 1) same downflow before and after pumping began

Case 2) no prepumping vertical flow and a maximum vertical flow after pumping began

Case 3) estimated prepumping downflow rate of $\sim 4.0 \times 10^{-7}$ cm/sec and an increased downflow after pumping

Tm = measured temperature

Tc = calculated temperature

q = vertical specific discharge (during pumping)

qo = vertical specific discharge (before pumping)

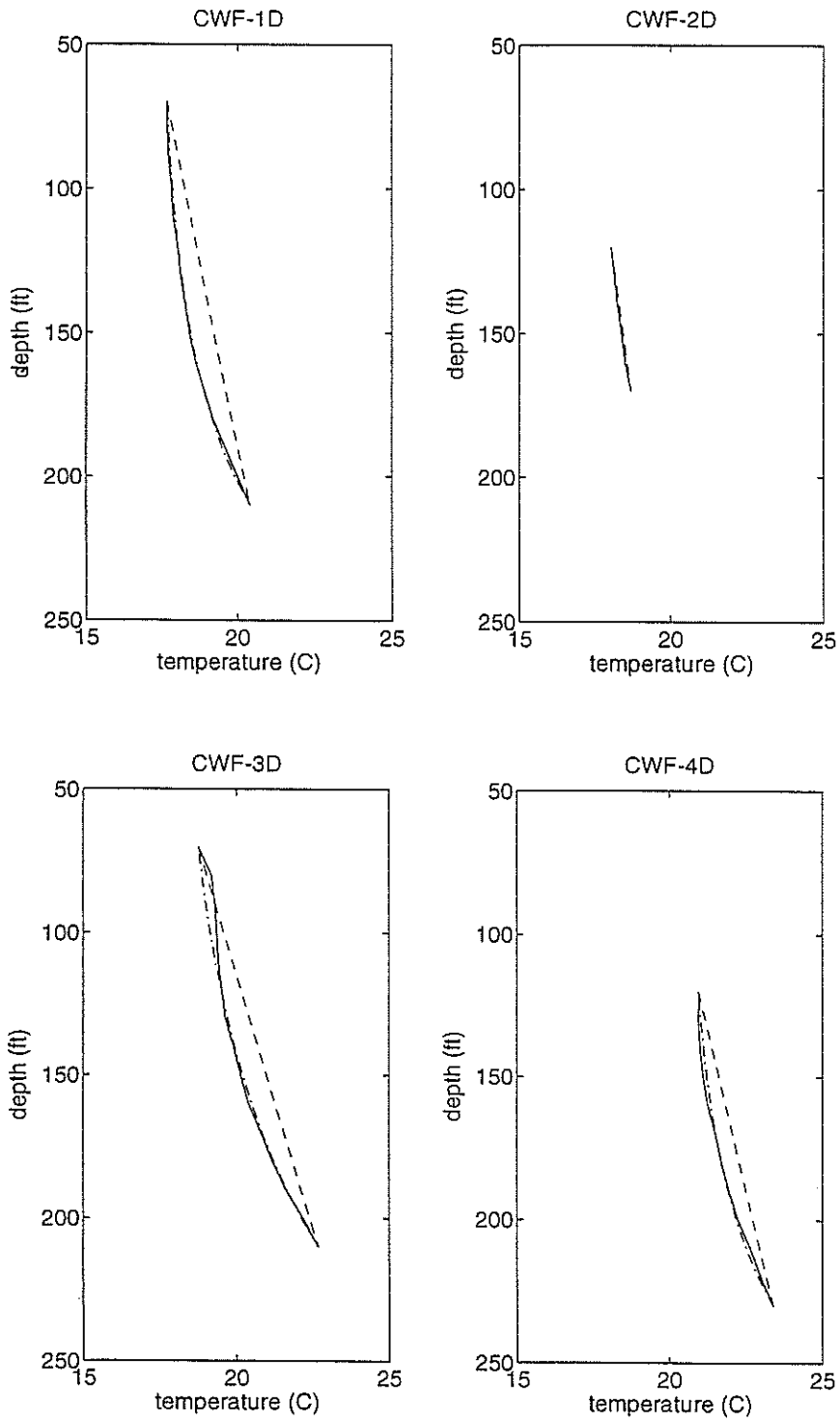

FIGURE 6. Upper flow zone, Case 2 (no initial vertical flow and a maximum vertical flow after pumping began; see text).
——— measured temperatures
- - - - - - - estimated initial temperatures
-·-·-·-·- calculated 1986 temperatures

to 1986. The prepumping downflow rate was derived from the difference between water levels in the first wells drilled in the upper and intermediate aquifers and from the effective hydraulic conductivity of the aquifers and clay layers. The temperatures for Case 3 are shown in Figure 7. The calculated downflow rates were effectively the same for all three cases. It should be noted that these results are based on the assumption that the temperatures at the top and bottom of the zone are constant in time.

As can be seen by comparing Tables 4 and 5, the pumping schedule estimates of downflow in the upper flow zone were somewhat greater than those flows estimated using the computer model for the case of maximum during-pumping downflow (Case 2; Table 2). Had we used the downflow estimates from the pumping schedules in the computer model, we would not have been able to fit the measured temperatures (assuming prepumping flow was zero or downward as per head data). The specific discharge from the upper to lower intermediate zones may have been overestimated with the pumping schedule correlations either because we overestimated the effective hydraulic conductivities or the head differences.

Deep flow zone (lower intermediate to deep aquifer)

Flow rates from the lower intermediate aquifer to the deep aquifer for the three cases discussed above are summarized in Tables 6, 7, and 8. In the first case, the minimum prepumping upflow case, there was no downflow for the 30 years of pumping, that is, the temperatures were allowed to only diffuse to their 1986 values (Table 2). The prepumping minimum upward discharge ranged from 6.0×10^{-7} cm/sec in Well CWF-1D to 1.6×10^{-7} cm/sec in Well CWF-4D (Table 6). The initial established temperatures, the decayed curves, and the measured temperature data for this case are shown in Figure 8.

The prepumping upward flows for the second case (maximum prepumping upflow

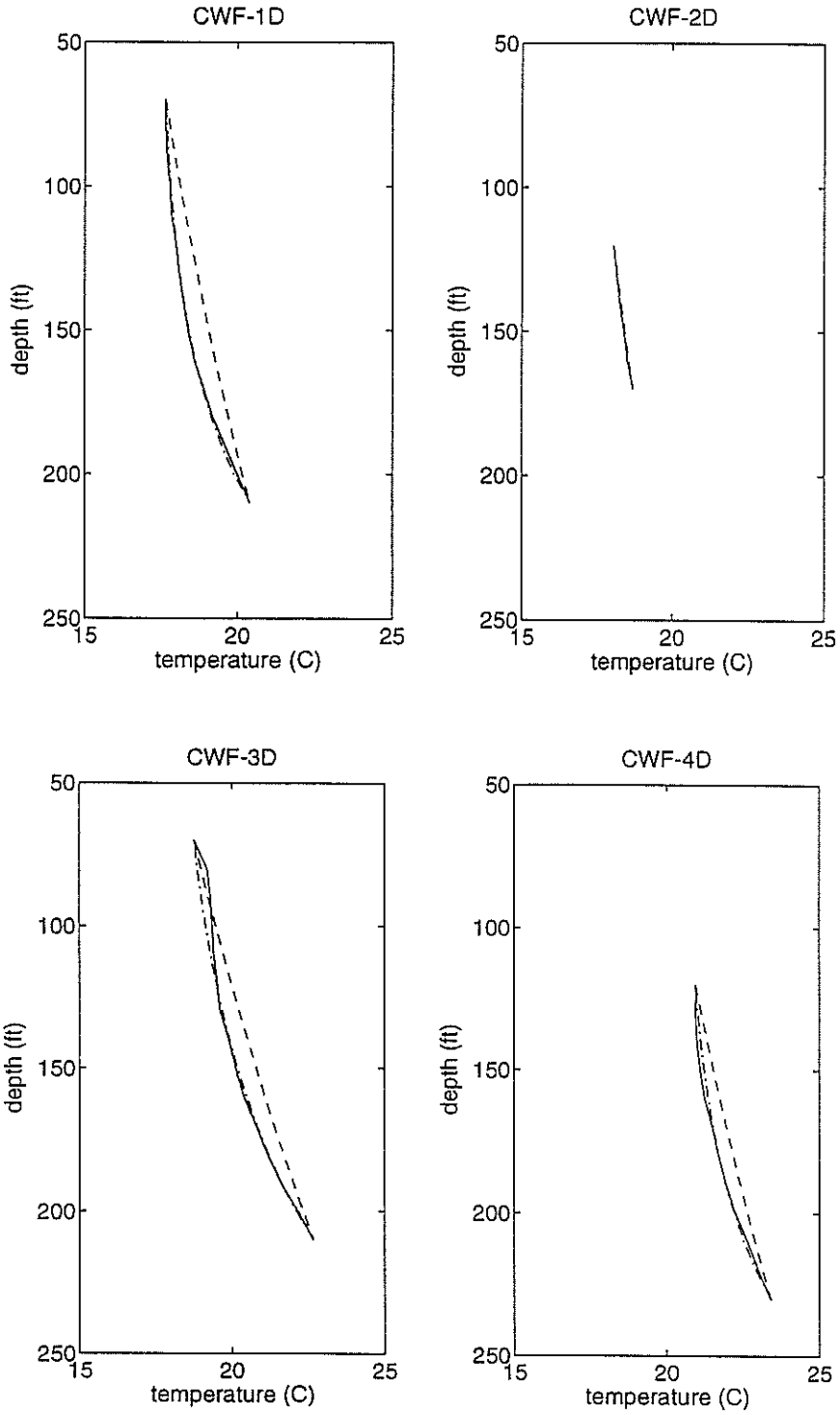

FIGURE 7. Upper flow zone, Case 3 (estimated prepumping downflow rate of ~4.0 x 10^{-7} cm and increased downflow after pumping began; see text).

——— measured temperatures

- - - - - - - estimated initial temperatures

-·-·-·-·- calculated 1986 temperatures

TABLE 6. Deep flow zone (flow from lower intermediate to deep aquifers). Case 1: Minimum prepumping upflow and no vertical flow during pumping.

Well	Zone (depth, feet)	qo (cm/sec)	q (cm/sec)	Sum of squares
1D	210-800	-6.0×10^{-7}	0.0	5.64
2D	170-790	-5.3×10^{-7}	0.0	18.0
3D	210-790	-4.3×10^{-7}	0.0	6.86
4D	230-790	-1.6×10^{-7}	0.0	1.35

qo = vertical specific discharge (before pumping)
q = vertical specific discharge (during pumping)

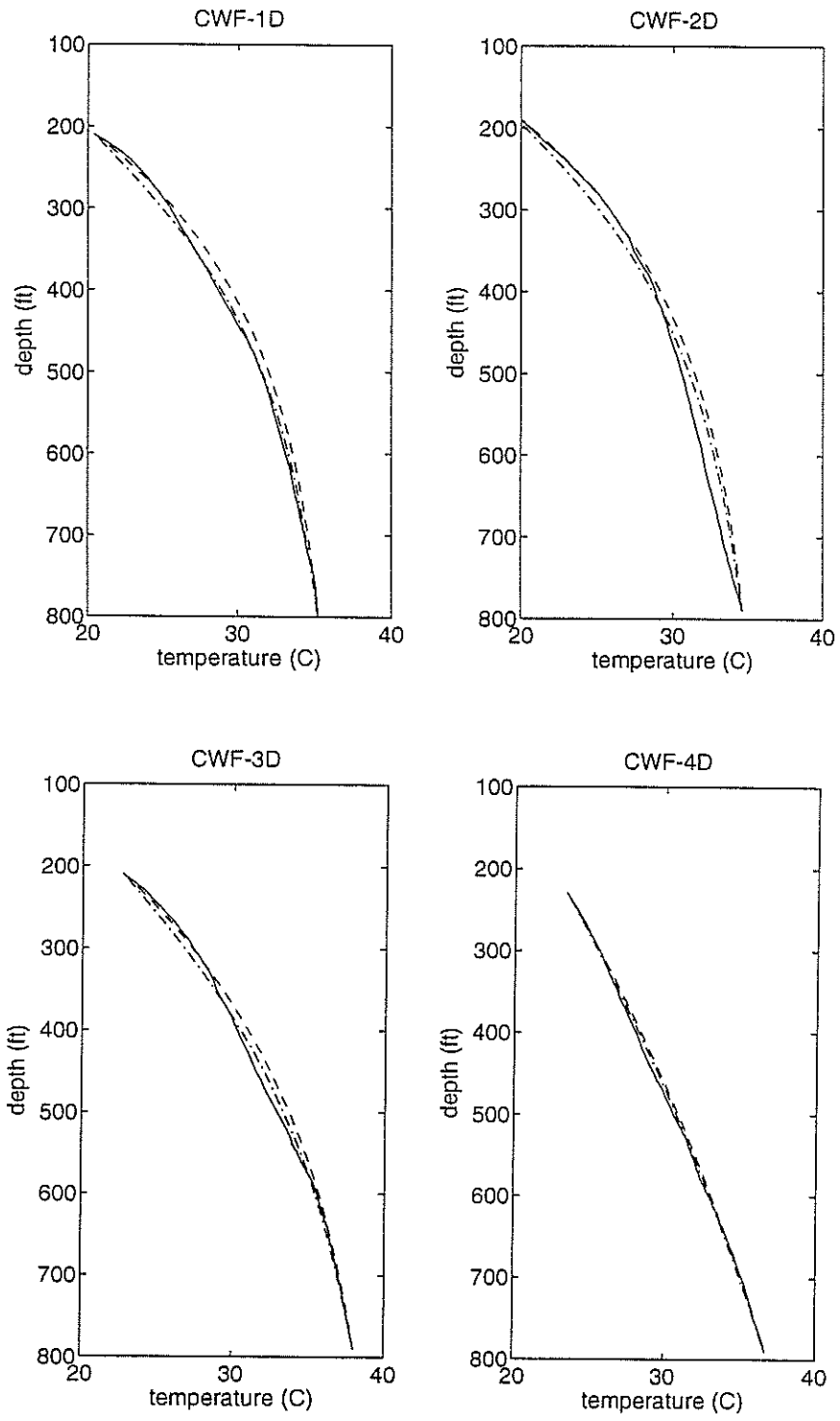

FIGURE 8. Deep flow zone (lower intermediate to deep aquifer), Case 1 (Table 2)

——— measured temperatures

- - - - - - - estimated initial temperatures

-·-·-·-·-·- calculated 1986 temperatures

TABLE 7. Deep flow zone (flow from lower intermediate to deep aquifer). Case 2: Maximum prepumping upflow and one value of maximum downflow below ~300 feet over 30 years of pumping.

Well	Zone (depth, feet)	qo (cm/sec)	q (cm/sec)	Total sum of squares for both zones
1D	210-300	-2.2×10^{-6}	0.0	
	300-800	-2.2×10^{-6}	5.9×10^{-6}	7.9
2D	170-370	-8.5×10^{-7}	0.0	
	370-790	-8.5×10^{-7}	4.4×10^{-6}	5.1
3D	210-330	-8.5×10^{-7}	0.0	
	330-790	-8.5×10^{-7}	2.9×10^{-6}	2.1
4D	230-310	-2.2×10^{-6}	0.0	
	310-790	-2.2×10^{-6}	8.8×10^{-6}	8.1

qo = vertical specific discharge (before pumping)
q = vertical specific discharge (during pumping)

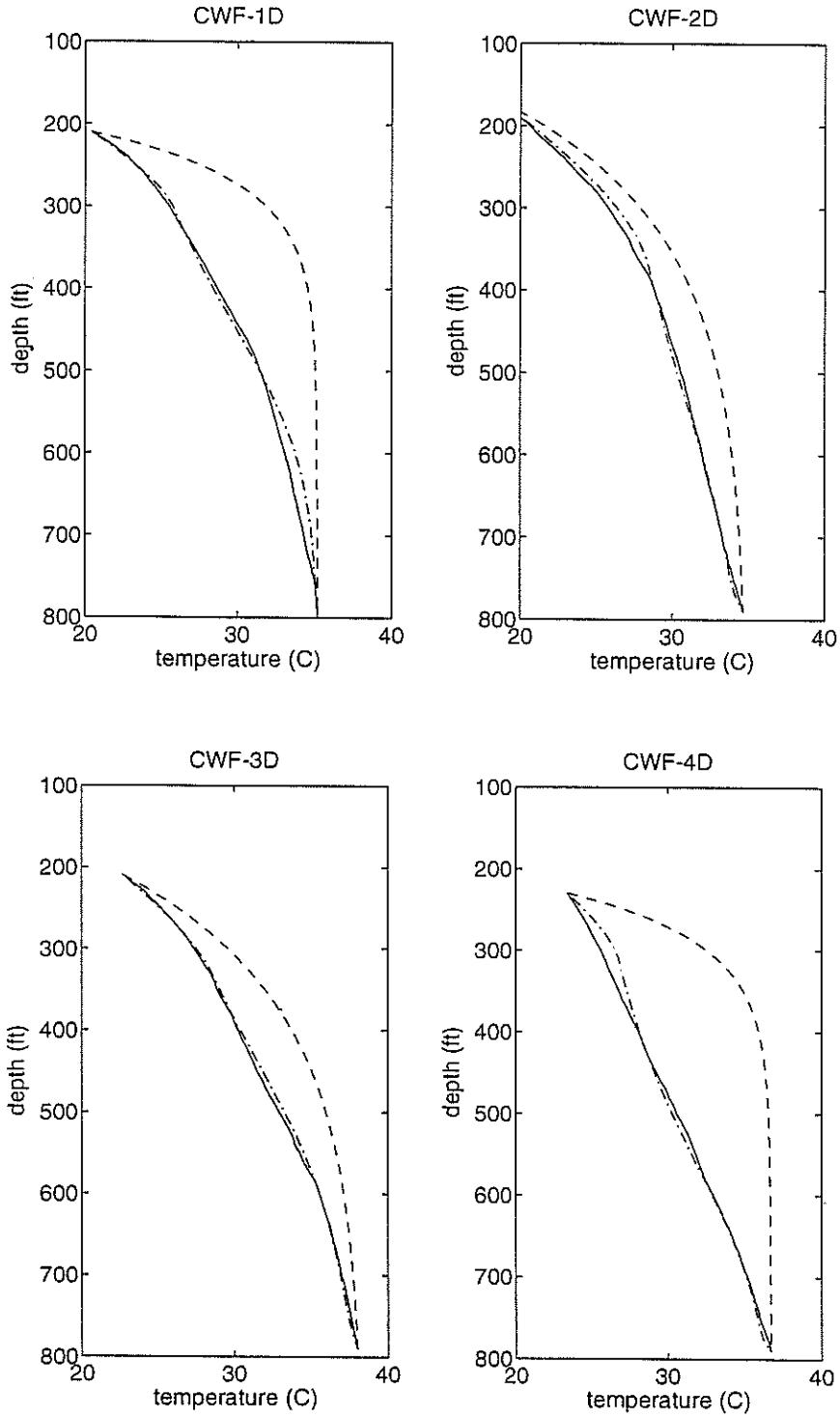

FIGURE 9. Deep flow zone, Case 2 (Table 2)
——— measured temperatures
- - - - - - estimated initial temperatures
-·-·-·-·- calculated 1986 temperatures

Table 8. Deep flow zone (flow from lower intermediate to deep aquifer). Case 3: Downflow during pumping equal to vertical flow estimated from pumping schedules.

Well	Zone (depth, feet)	qo (cm/sec)	q (cm/sec)	Total sum of squares for both zones
1D	210-300	-9.0×10^{-7}	0.0	6.3
	300-800	-9.0×10^{-7}	1.7×10^{-6}	
2D	170-370	-6.0×10^{-7}	0.0	8.0
	370-790	-6.0×10^{-7}	1.1×10^{-6}	
3D	210-330	-5.4×10^{-7}	0.0	5.2
	330-790	-5.4×10^{-7}	7.9×10^{-7}	
4D	230-310	-4.0×10^{-7}	0.0	1.7
	310-790	-4.0×10^{-7}	1.7×10^{-6}	

qo = vertical specific discharge (before pumping)
q = vertical specific discharge (during pumping)

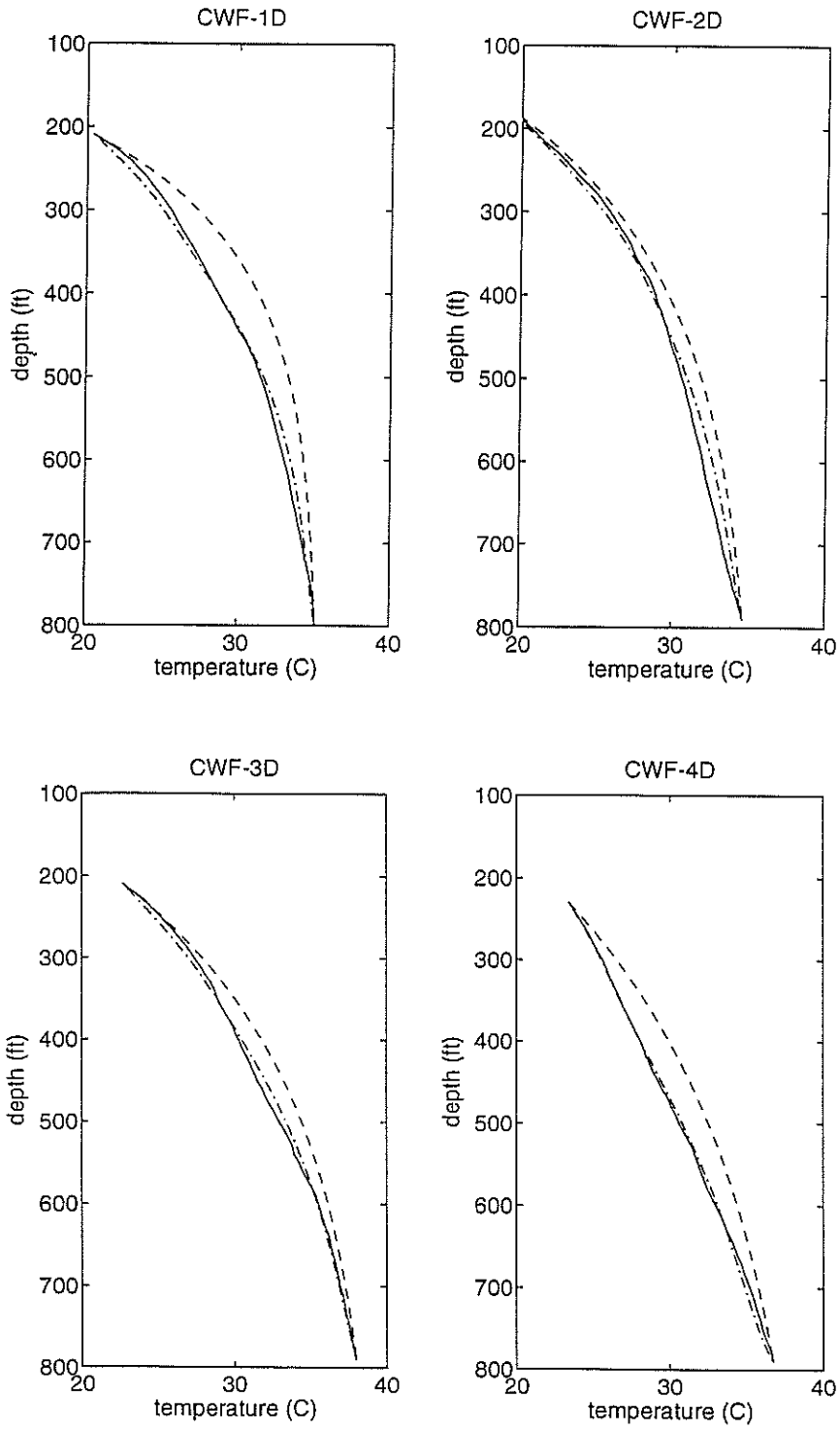

FIGURE 10. Deep flow zone, Case 3 (Table 2)
——— measured temperatures
- - - - - - - estimated initial temperatures
-·-·-·-·-·- calculated 1986 temperatures

with one maximum downflow rate below 300 feet during pumping, and no vertical flow from 200 to 300 feet during pumping; Table 2) were somewhat greater than those in Case 1 for all the wells (Table 7). The during-pumping downflow rate for this case was the calculated maximum downflow that would occur across the clay layer if a maximum head drop occurred across only the clay layer. This maximum downflow rate was then applied over the entire depth zone. The estimated prepumping upflow rates, as well as the calculated during-pumping downflow rates are listed in Table 7. The final calculated temperatures with the estimated initial temperatures and the measured temperatures are shown in Figure 9.

In the third case (Table 2), a prepumping upward specific discharge before pumping was estimated from the computer model by assuming the downflow from about 300 to 800 feet depth during 1956 to 1986 was the 30-year downflow estimated from pumping information (Table 4). As in Case 2 there was no vertical flow from ~200 to ~300 feet. The prepumping upward flows ranged from -4. x 10^{-7} cm/sec in Well-4D to -9. x 10^{-7} cm/sec in Well-1D (Table 8). The downflow rates during pumping for Case 3 are between those rates calculated in Cases 1 and 2 for all the wells (Tables 6, 7, and 8). The initial established temperatures, the final calculated temperatures, and the measured temperature data for this case are shown in Figure 10.

STEADY-STATE MODEL AND CONDUCTIVE-ADVECTIVE ENERGY BALANCE

If temperatures are steady-state, the change in advected heat across the groundwater flow zone should equal the change in conducted heat across the zone:

$$Q_2 - Q_1 = \rho c \, q_z \, (T_2 - T_1) \, . \qquad (9)$$

In most cases these heat flow changes will not be equal but will differ by some residual amount, ΔQ_R:

$$\Delta Q_R = (Q_2 - Q_1) - \rho c\, q_z\, (T_2 - T_1) \; . \qquad (10)$$

This energy consideration provides a means of qualitatively evaluating how reasonable a steady-state model is for the temperature profile.

The flow rates calculated from the steady-state model (using the heat flow-temperature data) for the zones in each of the four wells were used to estimate the change in advected heat across each of the depth zones described above (Table 9). The conductive heat flow values listed in Tables 13–16 were used to calculate the conductive heat-flow change across each zone. The amount by which these heat-flow changes differed, ΔQ_R, as a percent of the change in conducted heat is also shown in Table 9.

Advective and conductive heat flow changes agreed well for the upper part of well CWF-1D with only an 12% difference. The heat flow changes in the lower part of well CWF-1D were calculated with and without heat flow values at 240 and 260 feet depth. These two heat flow values did not lie on the Q versus T line with the other heat flow values (Figure 4). The agreement of advective and conductive heat flow changes was 22% or 13% (depending on whether depths 240 and 260 were included). Both the Q versus T plot and the difference in heat flow changes may suggest some flow not recognized in our steady-state model.

The percent difference between advective and conductive heat flow change across the upper flow zone in well 2D was 42% (Table 9). The heat flow changes across the second flow zone in well CWF-2D (190-600 feet) agreed fairly well with a residual of 28%. The

heat flow changes across the third zone of well-2D agreed well, 8%. The measured temperatures in the bottom zone will therefore not be well approximated by our transient model because we assume only downward flow in the deep zone during pumping, that is, notice in well 2D upflow from 790-600 feet is suggested from Q vs T plots (Figure 4).

The difference in advective and conductive heat flow change for the first (70-230 feet) and second (230-790 feet) zones of well CWF-3D were less than the difference in advective and conductive heat flow changes for the first and second zones of wells 1D and 2D. The residual heat flow changes were 10% and 16%, respectively.

Heat flow changes in the first (110-220 feet), second (220-280 feet), and fourth (510-790 feet) zones of well CWF-4D agreed fairly well, with percent residuals of 9%, 12%, and 32%, respectively. The heat flow change residual in zone three (280-510 feet) was very high. One may note from the conductive heat flow versus temperature plot (Figure 4) the values for zone two (280-510 feet) were scattered. It is therefore difficult to obtain representative conductive and advective heat flows for the zone; also small discrepancies in conduction and convection will generate large percentage errors in ΔQ_R because of the small changes in conductive and convective heat flows (Table 9).

The heat flow changes for the deep flow zone (well CWF-4D) did not agree quite as well when one flow was calculated for the entire zone (220-790 feet depth). The heat flow residual was 39% (Table 9). However in this case the zone with a very high residual (280-510 feet, $\Delta Q_R = 120\%$) was incorporated. The correlation coefficients for flow in the deep zone for well CWF-4D were somewhat lower than for the other wells (Table 1) so the calculated advective heat flows have a higher degree of uncertainty.

In summary the measured temperatures, in wells 1-4, generally support the steady-state model modestly well (i.e., $\Delta Q_R \leq 42\%$). In only one zone the measured

TABLE 9. Energy balance of measured temperatures based on specific discharge estimated from heat-flow plots.

Well	Zone (depth, feet)	ΔQcond (mW/m^2)	ΔQadv (mW/m^2)	%ΔQr: $\frac{\lvert \Delta Qcond - \Delta Qadv \rvert}{\Delta Qcond}$
1D	70-230	432	484	12%
	230-800	-294	-228	22%
	270-800	-194	-168	13%
2D	110-170	50	71	42%
	190-600	-236	-301	28%
	600-790	38	41	8%
3D	70-230	344	380	10%
	230-790	-194	-163	16%
4D	110-220	197	180	9%
	220-280	-58	-51	12%
	280-510	5	11	120%
	510-790	-82	-56	32%
	220-790	-103	-63	39%

temperatures yield % ΔQ_R which is quite large (>100%; Table 9). With the exception of Well CWF-2D, the advective and conductive heat flow changes across the upper downflowing portion of the temperature curve agreed to within 12%. For the upper zone in well CWF-2D the % ΔQ_R was 42%. The steady-state temperature model in general supports the concept of steady downward flow in the upper flow zone. For the deep flow zone the steady-state temperature model supports the idea of the temperature profile curvature being caused by mostly upward prepumping groundwater flow, possibly with some secondary components (transient temperatures or horizontal temperature gradients).

CONDUCTIVE-ADVECTIVE ENERGY BALANCE FOR ESTIMATED INITIAL TEMPERATURES OF COMPUTER MODELS

The estimated initial temperatures for the computer model are in essence initial conditions for those models and may be thought of as steady-state. Therefore, the change in advective and conductive heat flow as determined from the estimated initial temperatures should balance across each groundwater flow zone as for the steady-state cases based on the measured heat flow-temperature plots. The conductive and advective heat flow changes as well as the percent residual heat flow for Case 1 and Case 3 of the upper flow zone and Cases 1, 2 and 3 of the lower water flow zones are listed in Table 10 (see Table 2 for case descriptions). Initial temperatures for Case 2 of the upper water flow zone (no vertical groundwater flow prior to 1986) lay on a linear temperature gradient so the conductive and advective heat flow changes for this case were not included (they both would have been zero).

The heat flow change residuals, ΔQ_R, for the estimated initial temperatures of Cases 1 and 3 of the upper groundwater flow were between 7 and 27% in all four wells. Advective

and conductive heat flow changes also balanced quite well in the deep flow zone for all three cases at all four well sites. ΔQ_R was generally less than 10%. These results show that the estimated initial temperature profiles closely approximate steady-state temperatures.

COMPARISON OF TRANSIENT AND STEADY-STATE RESULTS

The during-pumping vertical flow rates estimated for the upper flow zone with the transient numerical model were roughly equal to the rates calculated assuming a steady-state temperature model at Sites 1 and 3 (Table 11). The downflow rates estimated with the computer model at site 2 were slightly less than the steady-state temperature estimates, while the computer model downflow estimates at site 4 were slightly greater than steady-state estimates.

Prepumping vertical specific discharges estimated for the deep flow zone from both the steady-state and transient models are compared in Table 12. In Case 1 there is reasonably good agreement between the estimates of prepumping flow. At well sites 1 and 4, estimates of initial (or prepumping) upflow using Case 2 (computer model; Table 2) differ from the steady-state model estimates of upflow by factors of ~4 - 20. The prepumping upflow estimates for Case 3 (intermediate downflow during pumping) ranged from being roughly equal to the steady-state estimates to being roughly four times greater than the steady-state estimates. Flow rates for Cases 1 and 3 agreed with each other much better than with Case 2.

UNCERTAINTY

Steady-state model

Errors in the vertical specific discharge values calculated with the steady-state model

TABLE 10. Energy balance of initial (prepumping) temperatures estimated with transient model.

Well	Zone (depth, feet)	Case	ΔQcond (mW/m^2)	ΔQadv (mW/m^2)	ΔQ_r: $\frac{\lvert \Delta Qcond - \Delta Qady \rvert}{\Delta Qcond}$
1D	70-210	1	236	265	12%
	70-210	3	43	46	7%
	210-800	1	-360	-370	3%
	210-800	2	-1250	-1358	9%
	210-800	3	-547	-567	4%
2D	120-170	1	41	52	27%
	120-170	3	9	11	22%
	170-790	1	-344	-354	3%
	170-790	2	-547	-567	4%
	170-790	3	-389	-400	3%
3D	70-210	1	239	262	10%
	70-210	3	53	57	8%
	210-790	1	-269	-276	3%
	210-790	2	-526	-546	4%
	210-790	3	-337	-347	3%
4D	120-230	1	216	246	14%
	120-230	3	37	41	11%
	230-790	1	-87	-89	2%
	230-790	2	-1127	-1224	9%
	230-790	3	-217	-223	3%

*note: Case 1) upper flow zone—same downflow before and during pumping
Case 3) upper flow zone–estimated original downflow of $\sim 4 \times 10^{-7}$ cm/sec
Case 1) deep flow zone—minimum prepumping upflow
Case 2) deep flow zone—maximum prepumping upflow
Case 3) deep flow zone—downflow during pumping equal to flow estimated from pumping schedules

are due to uncertainties in the temperature data, uncertainties in thermal conductivities of aquifer material, and uncertainties of in situ porosities of the aquifer system. The major error in the temperature data is probably the reading precision from the temperature log ($\pm$.025°C). This uncertainty is small compared to the uncertainty contributed by the other factors. Thermal conductivities of well cuttings measured by the method described above are accurate to about $\pm$10%-15% (Deming et al. 1992); however, the porosity values are probably only accurate to $\pm$20% (i.e., 7% variation in 35% porosity). The accuracy of the heat flow values is therefore about $\pm$20%.

In addition to the error associated with uncertainty in the porosity values read from the neutron logs there may be errors caused by not knowing the correct calibration scale for the logs. These errors would be approximately the same for all of the depths, however (representing a shift in the porosities), and since the specific discharge was calculated from a difference in heat flows this error should not greatly affect the calculated specific discharge values.

Transient model

Errors in the temperatures calculated with the finite-difference scheme are a result of truncation errors arising from ignoring higher order terms in the Taylor series from which the finite-difference method was derived. Since the method is centered in space but forward in time the local truncation error will be of order O ($\Delta t + \Delta z^2$) (Burden and Faires 1989). A comparison of the analytical solution detailed in Appendix B with the numerical solution indicates that the numerical solution converges to the analytical solution for long time or steady-state solutions. This result suggests that the truncation errors in the numerical solution are not significant. The stability of the transient solution was discussed above. The vertical

TABLE 11. Comparison of downflow rates during pumping in upper zone estimated from steady-state and transient models.

Well	Zone (depth, feet)	Steady-state downflow (cm/sec)	Computer modeled during-pumping downflow (cm/sec)		
			Case 1	Case 2	Case 3
1D	~70-210	2.6×10^{-6}	2.3×10^{-6}	2.5×10^{-6}	2.5×10^{-6}
2D	~120-170	2.6×10^{-6}	1.9×10^{-6}	2.0×10^{-6}	1.9×10^{-6}
3D	~70-210	1.7×10^{-6}	1.6×10^{-6}	1.7×10^{-6}	1.7×10^{-6}
4D	~120-230	2.1×10^{-6}	2.4×10^{-6}	2.5×10^{-6}	2.4×10^{-6}

*note:

Case 1) upper zone—same downflow before and during-pumping
Case 2) upper zone—no prepumping downflow
Case 3) upper zone—estimated prepumping downflow of $\sim 4 \times 10^{-7}$ cm/sec

TABLE 12. Comparison of prepumping upflow rates in deep flow zone (lower intermediate to deep aquifers) estimated from steady-state and transient models.

Well	Zone (depth, feet)	Steady-state upflow (cm/sec)	Computer modeled prepumping downflow (cm/sec) Case 1	Case 2	Case 3
1D	230-800	-4.2×10^{-7}			
	270-800	-3.7×10^{-7}			
	210-800	—	-6.0×10^{-7}	-2.2×10^{-6}	-9.0×10^{-7}
2D	210-600	-6.0×10^{-7}			
	170-790	—	-5.3×10^{-7}	-8.5×10^{-7}	-6.0×10^{-7}
3D	230-790	-2.8×10^{-7}			
	210-790	—	-4.3×10^{-7}	-8.5×10^{-7}	-5.4×10^{-7}
4D	220-280	-6.1×10^{-7}			
	510-790	-2.3×10^{-7}			
	220-790	-1.1×10^{-7}			
	230-790	—	-1.6×10^{-7}	-2.2×10^{-6}	-4.0×10^{-7}

*note:

Case 1) deep zone—minimum prepumping upflow (Table 2)

Case 2) deep zone—maximum prepumping upflow (Table 2)

Case 3) deep zone—downflow during pumping equal to flow estimated from pumping schedules

specific discharge and the time increment were chosen to insure that the solutions would be stable.

CONCLUSIONS AND RECOMMENDATIONS

If the horizontal temperature gradient is insignificant at the Cañutillo site (so that horizontal water flow has not significantly affected the subsurface temperatures) the transient temperature model suggests the prepumping upward water flow from the deep to lower intermediate aquifer was between -1.6 x 10^{-7} cm/sec and -2.2 x 10^{-6} cm/sec (Table 12). The steady-state model gave vertical specific discharge rates within this range except for two short zones of downward flow at wells sites 2D and 4D (Table 1). The during-pumping downward flow from the upper to the lower intermediate aquifers estimated using the transient model was between 1.6 x 10^{-6} and 2.5 x 10^{-6} cm/sec (Table 11). The steady-state model gave vertical discharge rates nearly equal to the transient temperature model estimates. We can conclude therefore that steady-state interpretation of the temperature data does not greatly conflict with the results obtained from the transient model for prepumping vertical flow from the deep to the lower intermediate zone and for during-pumping flow from the upper to the lower intermediate zone.

The temperature data in the deep flow zone (lower intermediate and deep aquifer) are the result of either diffusion of an initial temperature distribution in the case of minimum prepumping upflow or some combination of advective and diffusive cooling of an initial temperature distribution. Cases 2 and 3 (Table 2) for downward flow in the lower intermediate and deep aquifers suggest an upper region within the deep flow zone without vertical flow (from about 200 to 300 feet) and a region from ~300 to 800 feet depth with downward groundwater flow. Case 3 (deep flow zone; Table 2), which we believe to be the

most realistic interpretation of the flow history in the aquifer system, suggests that the downward flow in the deep flow zone is presently 45-325% greater than the past (prepumping) upward flow (Table 8).

The major unanswered questions in this study are the influence of horizontal temperature gradients on the vertical temperature distributions and whether the boundary temperatures varied with time. To answer the first question information must be obtained about the horizontal temperature distribution in the area. The second question could be addressed by measuring temperatures over a greater depth range, from shallower to deeper depths, more likely to be bounded by regions of little or no groundwater flow.

There are several observation wells to the north, south and west of wells CWF-1D - CWF-4D in the Cañutillo well field. Temperature logs could be taken in these observation wells to provide more information about horizontal as well as vertical temperature distributions in the well field. The transient temperature model could be modified to account for horizontal temperature gradients. Temperature logs in the shallow piezometers (CWF-1-4A) as well as temperature logs from a deep observation well (CR-2 1050 feet depth) would provide temperature data over a greater depth range.

SUMMARY

By making assumptions about prepumping downflow in the upper flow zone we estimated, with a computer model, a range of downflows during pumping (the model was a finite-difference approximation to the one-dimensional advective-diffusion equation). The during-pumping downflow estimates ranged from 1.5×10^{-6} to 2.5×10^{-6} cm/sec (Table 11). By making assumptions about downflow during pumping in the deep flow zone we estimated, with the computer model, a range of prepumping upflows. Most of the prepumping upflow

estimates ranged from 4. x 10^{-7} to 9. x 10^{-7} cm/sec (Table 12). These estimates of during-pumping downflows in the upper flow zone and prepumping upflows in the lower flow zone were similar to estimates of the vertical component of flow calculated from heat flow data assuming a steady-state temperature model (Tables 11 and 12). This preliminary result suggests that pumping of the well field for 30 years has not made an overwhelming impact on the temperature distribution in the aquifer system. In the deep flow zone it appears possible that downward flow is currently (45-325%) greater than the prepumping upflow (Table 8). Our best estimates of during-pumping downflow in the upper flow zone suggest that downflow has possibly increased 500% as a result of pumping (estimates of ground-water flow in both the upper and deep flow zones are based upon uncertain head and interpreted production data, so these conclusions should be further substantiated).

This study has shown that temperature data can be used under certain conditions to estimate the prepumping vertical component of flow in an aquifer system if sufficient information is available about vertical flow during pumping; alternatively, the average vertical component of flow during pumping can be estimated when sufficient information is available about prepumping vertical flow rates.

APPENDIX A

COMPUTER PROGRAMS

```
      program transfour
c
c     Program transient-four uses the Forward Euler method to approximate
c     the advection-diffusion equation for transport of heat by conduction
c     and water movement in an aquifer. The thermal diffusivity, kt, is
c     assumed to be constant in space and time. The time increment, dt,
c     and the space increment, dz, are fixed at 1,000,000 sec and 10 feet
c     but can be easily changed. This version of transient allows
c     the total depth to be divided into either two or four subzones with
c     different darcian velocities. The velocity is constant within each
c     zone.
c
c                          Variables
c
c                  i  = time counter
c                  j  = space counter
c                  n  = initial data counter
c                  k  = number of time steps
c                  m  = number of depths
c                  l  = number of depths to the base of a subzone
c                  p  = number of depths to the base of a subzone
c                  q  = number of depths to the base of a subzone
c                  dz = spatial step = 304.8 cm
c                  dt = time step = 1,000,000 seconds
c                  kt = thermal diffusivity
c                   c = ratio of the product of specific heat and density
c                       of water to the specific heat and density of the
c                       saturated aquifer
c                  kp = total amount of time
c                  x1 = current temperature at i,j
c                  x2 = advective term
c                  x3 = diffusive term
c                  d# = depth interval of subzones
c                  v  = darcian velocity
c                  z  = (mx1) matrix of depths
c                  T  = (mxk) matrix of temperatures
c
      integer i, j, n, k, m, l, p, f, q
      real dz,v, c, kt,kp,x1, x2, x3, dt,d1,d2,d3,d4,d5

c     up to 150 spatial and 5000 temporal steps are allowed
      dimension T(150,5.E+3),z(150)
      character*20 indat, outdat

c     space increment, time increment and aquifer properties are fixed
```

```
      parameter (dz = 304.8, c = 1.1,dt = 1.0E+6, kt = 4.41E-3)

c     data files are chosen-the data file should contain the depths in
c     one column and the temperatures in the second column

      write(6,*)'enter input and output file names'
      read(5,*)indat, outdat
      open(unit =12,file =indat)
      open(unit = 13, file = outdat)

c     number of zones of constant darcian velocity are choosen

      write(6,*)'enter the number of flow zones (2 or 4)'
      read(5,*) f

c     for this option (f=2) the top flow zone has v set equal to zero
c     and the user inputs v for the lower flow zone

      if(f.eq.2)then

c     the user inputs the depth intervals and the total amount of time

      write(6,*)'enter d1, d2, d3 and time (cgs units)'
      read(5,*)d1,d2,d3,kp
      write(6,*)'enter vertical flow'
      read(5,*)v

c     the number of depth intervals in each subzone are calculated

      l = ((d2-d1)/10)+1
      m = ((d3-d1)/10)

c     the number of time steps is calculated

      k = abs(kp/dt)
      write(6,*)k,dt

c     the data are read from the input file, these are the temperatures
c     at time t = 0.

      do 150 n = 0,m

          read(12,*) z(n), T(n,0)
150   continue

c
c     the temperatures are calculated at each time step based on the spatial
```

```
c     gradients of the previous times step.
c
      do 300 i = 0,k
c
c     the temperatures at the top and bottom are fixed at their time = 0.0
c     value
c
         T(0,i) = T(0,0)
         T(m,i) = T(m,0)
         do 210 j = 1,l
c
c          zone of diffusion only
c
          x1 = T(j,i)
          x3 = kt*dt*(T(j+1,i)-2*T(j,i) + T(j-1,i))/(dz**2)
          T(j,i+1)= x1 + x3
 210     continue

         do 220 j = l,m-1
c
c        advective and diffusive terms
c
          x1 = T(j,i)
          x2 = - c*v*dt*(T(j+1,i)-T(j-1,i))/(2*dz)
          x3 = kt*dt*(T(j+1,i)-2*T(j,i) + T(j-1,i))/(dz**2)

         T(j,i+1) = x1 + x2 + x3
 220  continue
 300  continue
      else
c
c     for this choice (f=4) four depth zones are entered and the darcian
c     velocities are entered (v at the top is not necessarily 0)
c
      write(6,*)'enter d1,d2,d3,d4,d5 and time (cgs units)'
      read(5,*)d1,d2,d3,d4,d5,kp
      write(6,*)'enter v1,v2,v3,and v4'
      read(5,*)v1,v2,v3,v4
c
c     the number of spatial steps are again calculated
c
      l = ((d2-d1)/10) + 1
      p = ((d3-d1)/10) + 1
      q = ((d4-d1)/10)  + 1
      m = ((d5-d1)/10)
c
c     number of time steps
```

```
c
      k = abs(kp/dt)
      write(6,*)k, dt
c
c     data are read in
c
      do 350 n = 0,m

           read(12,*) z(n), T(n,0)
350   continue
c
c     the temperatures at the next time step are calculated
c     the temperature at the boundary point between two zones is
c     calculated with the velocity of the lower zone
c
      do 400 i = 0,k
         T(0,i) = T(0,0)
         T(m,i) = T(m,0)
      do 360 j = 1,l

           x1 = T(j,i)
           x2 = - c*v1*dt*(T(j+1,i)-T(j-1,i))/(2*dz)
           x3 = kt*dt*(T(j+1,i)-2*T(j,i) + T(j-1,i))/(dz**2)
          T(j,i+1)= x1 + x2 + x3
360     continue
        do 370 j = l,p

           x1 = T(j,i)
           x2 = - c*v2*dt*(T(j+1,i)-T(j-1,i))/(2*dz)
           x3 = kt*dt*(T(j+1,i)-2*T(j,i) + T(j-1,i))/(dz**2)

        T(j,i+1) = x1 + x2 + x3
370     continue

        do 380 j = p,q

           x1 = T(j,i)
           x2 = - c*v3*dt*(T(j+1,i)-T(j-1,i))/(2*dz)
           x3 = kt*dt*(T(j+1,i)-2*T(j,i) + T(j-1,i))/(dz**2)

        T(j,i+1) = x1+x2+x3
380     continue
        do 390 j = q,m

           x1 = T(j,i)
           x2 = - c*v4*dt*(T(j+1,i)-T(j-1,i))/(2*dz)
           x3 = kt*dt*(T(j+1,i)-2*T(j,i) + T(j-1,i))/(dz**2)
```

```
            T(j,i+1) = x1+x2+x3

 390      continue
 400      continue

          end if
c
c         the temperatures at the last time step are written
c         to the output file.  these temperatures are the approximate
c         solution to the advection-diffusion equation at that time
c
          do 500 i = 0,m

               write(13,*) z(i),T(i,k)

 500      continue
          stop
          end
```

```
      program transient

c     program transient solves the one-dimensional advection-diffusion equation
c     with the Forward Euler numerical approximation.  The aquifer thermal
c     properties are assumed to be constant in space and time.  The spatial
c     increment and temporal increment are also fixed but can be easily
c     changed.  The approximate solution at the final time step is written to
c     a data file that the user chooses.  The temperatures calculated at each
c     time step are not stored.
c
c                              Variables
c
c                     i  =  time counter
c                     j  = space counter
c                     n  = data counter
c                     m  = total number of space steps and initial data
c                     k  = total number of time steps
c                     T  = (mx1) matrix of temperatures
c                    dz  = spatial increment
c                    dt  = time increment
c                     c  = ratio of product of specific heat and density
c                          of water to product of specific heat and density
c                          of aquifer
c                    kt  = thermal diffusivity of aquifer
c                    kp  = total amount of time
c                     z  = depth a (mx1) matrix
c                     x1 = current temperature at i,j
c                     x2 = advective term
c                     x3 = diffusive term
c                     v  = darcian velocity
c                     Tp = top temperature
c                     Tm = bottom temperature
c
      integer i, j, n, k, m
      real  dz, v, c, kt, z, kp, dt
      double precision T, Tp, Tm, x1, x2, x3
c
c     a maximum of 100 spatial steps are possible; this can easly be modified
c
      dimension T(100),z(100)
      character*20 indat, outdat
c
c     the time and space increments are set as are the aquifer properties
c
      parameter (dz = 304.8, c = 1.1,dt = 1.0E+6, kt = 4.41E-3)
      write(6,*)'enter input and output file names'
c
```

```
c     the input and output files are specified by the user.  the input file
c     should have a column of depths and a column of temperatures
c
      read(5,*)indat, outdat
      open(unit =12,file =indat)
      open(unit = 13, file = outdat)
c
c     the user enters the darcian velocity, the total amount of time,
c     and the total number of depth points
c
      write(6,*)'enter velocity, time, (cgs units) and number of points'

      read(5,*)v, kp, m
      m = m-1
c
c     the number of time steps is calculated
c
      k = abs(kp/dt)
      write(6,*)k, dt
c
c     the data are read from the user specified file; these are the
c     temperatures at time = 0.0
c
     do 100 n = 0,m

         read(12,*) z(n),T(n)

 100  continue
c
c     the end temperatures are fixed at their time = 0 value.  this could
c     be modified to have the the boundary temperatures vary with time.
c
        Tp = T(0)
        Tm = T(m)
     do 300 i = 0,k
c
c     the temperatures are calculated at each time step based on the
c     gradients at the previous time step.  the temperatures at past
c     time steps are not preserved to minimize the amount of required
c     memory
c
        T(0) = Tp
        T(m) = Tm
        do 200 j = 1,m-1

          x1 = T(j)
          x2 = - c*v*dt*(T(j+1)-T(j-1))/(2*dz)
```

```
          x3 = kt*dt*(T(j+1)-2*T(j) + T(j-1))/(dz**2)

         T(j) = x1+x2+x3
 200      continue

 300      continue
c
c       the approximate solution at time = kp are written to the output file
c
        do 400 l = 0,m
             T(m)=Tm
             write(13,*) z(l),T(l)

 400    continue
        stop
        end
```

APPENDIX B

ANALYTICAL VERIFICATION

Diffusion equation

An analytical solution to the diffusion equation is available for the initial temperature distribution shown in Figure 11 (dotted line). A solution to Equation 3 (if $q_z = 0$) is

$$T(z,t) = \frac{T_1 z}{a} + \sum_{n=1}^{\infty} \frac{4T_1}{n^2\pi^2} \sin\frac{n\pi}{2} \sin\frac{n\pi z}{a} e^{-ct} \qquad (11)$$

where

$$c = \frac{K' n^2\pi^2}{a^2}$$

$$K' = \frac{K}{\rho_s c_s} .$$

and ρ_s = density of rock

c_s = specific heat of rock

K = thermal conductivity

a = thickness of rock layers.

This solution was derived to represent a slab of rock ($z > a/2$) at one temperature coming into contact with an upper slab of rock ($z < a/2$) with a linear temperature gradient. The temperature at the lower boundary of the lower slab and the upper boundary of the upper slab are constant though time.

The error contributed by the diffusive term in the numerical solution (calculated with the program TRANSIENT) can be estimated by comparing the analytical solution given by Equation 11 with the numerical solution for the same initial temperature distribution (Figure 11). The specific discharge in the numerical solution will be zero.

A comparison was made of the two methods at 30 years and 1268 years (Figure 11). The sum in Equation 11 was taken out to 21 terms because the computer calculated e^{-ct} as zero when n was greater than 21. The sum of the squares of the difference between the analytical and numerical solution for t = 30 years was .05; the sum of the squares for t = 1268 years was 0.002, so the diffusive term contributes a negligible error.

Steady-state advection diffusion equation

The steady-state advection-diffusion equation is .

$$\frac{dT}{dz} = \frac{K}{C_w \rho_w} \frac{d^2T}{dz^2} \tag{12}$$

where

T = temperature

z = depth

C_w = specific heat of water

ρ_w = density of water

K = thermal conductivity of aquifer

q_z = vertical specific discharge

The solution to this equation is

$$T = \frac{(e^{\frac{c_w \rho_w q_z z}{K}} - 1)\ (T_2 - T_1)}{(e^{\frac{c_w \rho_w q_z D}{K}} - 1)} + T_1 \tag{13}$$

where

T_1 = top temperature

T_2 = bottom temperature

D = total depth of flow zone

(Mansure and Reiter 1979).

A comparison was made between temperature profiles calculated with Equation 13 and long-term ($\sim$1200 years) temperature profiles calculated with equation 4 (finite-difference solution). The long-term finite-difference solutions were considered to be steady-state because there was little difference between solutions calculated at 1200 years and at 2400 years, that is, the temperatures were not changing with time so $\partial T/\partial t \simeq 0$. The steady-state temperatures calculated with the analytical solution and with the finite-difference solution were very nearly equal for both upflow and downflow (the sum of the squares of the difference between the two profiles was <0.1 for all flow rates considered). This result suggests that the numerical solution converges to the analytical solution so the truncation error associated with the numerical solution is not significant.

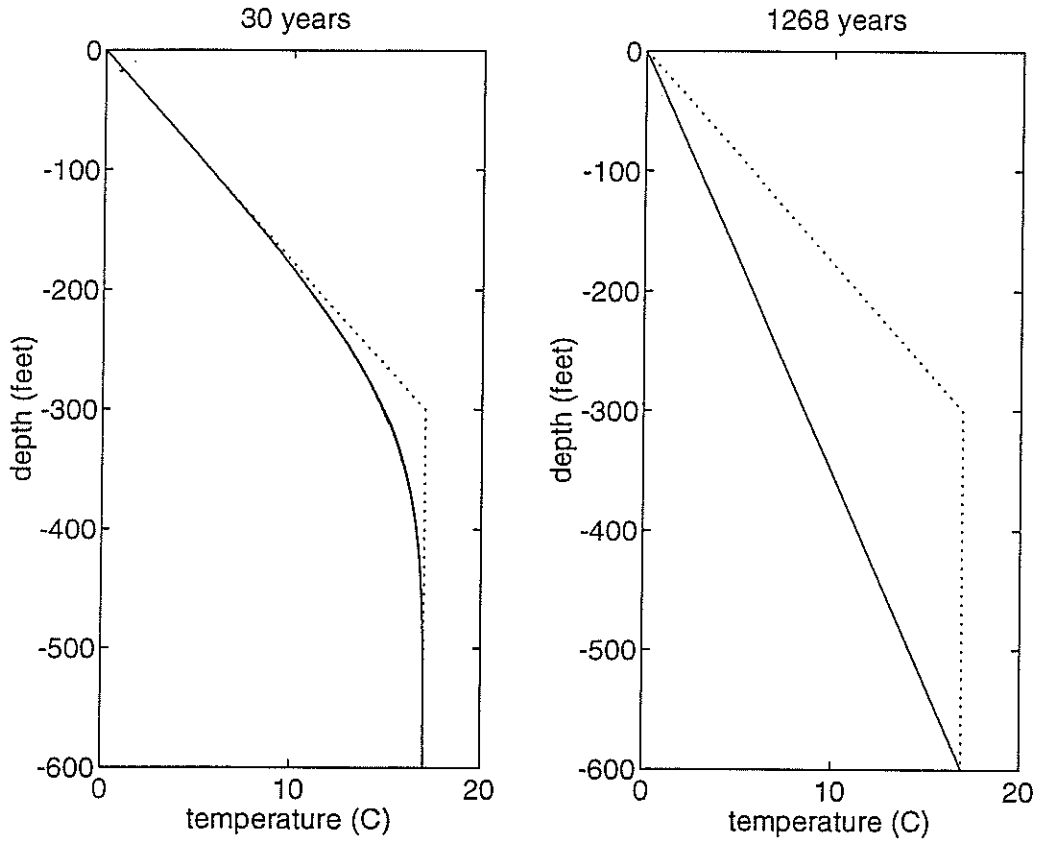

FIGURE 11. Comparison of numerical solution to analytical solution for diffusion of temperatures for 30 and 1268 years.

——— analytical solution

- - - - - - - numerical solution

. . . . . initial temperatures

APPENDIX C

THERMAL CONDUCTIVITY AND HEAT FLOW DATA

TABLE 13. Thermal conductivities and heat flow values for Well CWF-1D.

Depth feet	K_r mcal / cm-sec-C	ϕ	K_ϕ mcal / cm-sec-C	$\Delta T/\Delta z$ C / cm	Q mW / m^2
70-90	6.17	0.3	4.00	8.0×10^{-5}	13.7
90-110	6.20	0.29	4.08	2.5×10^{-4}	42.0
110-130	7.46	0.29	4.65	4.1×10^{-4}	79.8
130-150	6.49	0.275	4.31	4.9×10^{-4}	88.7
150-170	6.85	0.275	4.48	8.2×10^{-4}	153.7
170-190	5.66	0.31	3.72	1.15×10^{-3}	178.7
190-210	6.38	0.28	4.22	1.31×10^{-3}	231.7
210-230	5.60	0.285	3.82	2.79×10^{-3}	445.6
230-250	5.43	0.28	3.76	1.97×10^{-3}	309.6
250-270	6.14	0.285	4.08	1.56×10^{-3}	266.0
270-290	5.21	0.29	3.60	1.39×10^{-3}	210.0
290-310	6.39	0.29	4.16	1.15×10^{-3}	199.8
310-330	5.86	0.305	3.84	1.07×10^{-3}	171.3
330-350	6.75	0.305	4.23	1.15×10^{-3}	203.2
350-370	5.70	0.305	3.76	1.07×10^{-3}	167.7
370-390	5.34	0.32	3.53	9.8×10^{-4}	145.3
390-410	5.96	0.325	3.77	9.8×10^{-4}	155.2
410-430	5.67	0.325	3.65	1.07×10^{-3}	162.8
430-450	5.55	0.34	3.52	9.8×10^{-4}	144.9
450-470	6.50	0.35	3.85	9.8×10^{-4}	158.5
479-490	5.07	0.34	3.32	7.4×10^{-4}	102.5
490-510	7.00	0.34	4.11	6.6×10^{-4}	112.8
510-530	7.29	0.33	4.29	5.7×10^{-4}	103.0
530-550	5.22	0.325	3.45	4.9×10^{-4}	71.0
550-570	8.09	0.345	4.48	4.9×10^{-4}	92.2
570-590	6.99	0.35	4.04	4.9×10^{-4}	83.2
590-610	7.06	0.35	4.07	4.9×10^{-4}	83.8
610-630	7.98	0.34	4.48	4.1×10^{-4}	76.9
630-650	7.59	0.345	4.30	3.3×10^{-4}	59.0
650-670	8.03	0.335	4.54	4.1×10^{-4}	77.9
670-690	8.06	0.31	4.75	4.1×10^{-4}	81.5
690-710	7.99	0.315	4.68	3.3×10^{-4}	64.2
710-730	8.22	0.305	4.85	4.1×10^{-4}	83.2
730-750	6.93	0.27	4.55	4.1×10^{-4}	78.1
750-770	8.22	0.265	5.20	2.5×10^{-4}	53.5
770-790	7.77	0.32	4.55	8.0×10^{-5}	15.6
790-810	7.34	0.34	--	--	--

K_r - thermal conductivity of rock matrix
K_ϕ - in situ thermal conductivity (Sass et al. 1971).
ϕ - porosity
Q - heat flow

TABLE 14. Thermal conductivities and heat flow values for Well CWF-2D.

Depth feet	K_r mcal / cm-sec-C	ϕ	K_ϕ mcal / cm-sec-C	$\Delta T/\Delta z$ C / cm	Q mW / m^2
70-90	5.53	0.4	3.25	-1.6×10^{-4}	-21.8
90-110	6.42	0.39	3.60	-2.5×10^{-4}	-37.7
110-130	6.55	0.40	3.59	1.6×10^{-4}	24.0
130-150	6.60	0.40	3.61	4.1×10^{-4}	61.9
150-170	6.60	0.40	3.61	4.9×10^{-4}	74.0
170-190	7.75	0.35	4.32	2.10×10^{-3}	379.6
190-210	6.47	0.35	3.84	1.80×10^{-3}	289.2
210-230	5.46	0.35	3.44	2.10×10^{-3}	302.3
230-250	8.58	0.36	4.54	1.70×10^{-3}	322.9
250-270	6.95	0.36	3.96	1.80×10^{-3}	298.2
270-290	6.80	0.38	3.79	1.50×10^{-3}	237.9
290-310	6.90	0.38	3.82	1.20×10^{-3}	191.8
310-330	6.14	0.35	3.71	1.20×10^{-3}	186.3
330-350	5.96	0.38	3.49	8.2×10^{-4}	119.7
350-370	6.52	0.34	3.92	1.10×10^{-3}	180.4
370-390	5.21	0.34	3.38	9.8×10^{-4}	138.6
390-410	6.08	0.35	3.69	5.7×10^{-4}	88.0
410-430	6.72	0.38	3.76	6.6×10^{-4}	103.8
430-450	7.10	0.38	3.89	5.7×10^{-4}	92.8
450-470	7.53	0.37	4.10	5.7×10^{-4}	97.8
470-490	6.32	0.36	3.73	5.7×10^{-4}	89.0
490-510	5.49	0.36	3.41	5.6×10^{-4}	81.3
510-530	8.38	0.36	4.47	4.1×10^{-4}	76.7
530-550	6.54	0.37	3.76	4.1×10^{-4}	64.5
550-570	6.46	0.38	3.67	4.9×10^{-4}	75.2
570-590	5.78	0.38	3.43	4.9×10^{-4}	70.3
590-610	6.85	0.37	3.87	3.3×10^{-4}	53.4
610-630	6.61	0.36	3.84	4.1×10^{-4}	65.9
630-650	5.81	0.345	3.61	4.9×10^{-4}	74.0
650-670	6.38	0.345	3.84	4.9×10^{-4}	78.7
670-690	6.99	0.33	4.17	4.1×10^{-4}	71.5
690-710	7.52	0.32	4.45	3.3×10^{-4}	61.4
710-730	7.41	0.34	4.27	4.9×10^{-4}	87.5
730-750	8.19	0.345	4.52	4.9×10^{-4}	92.7
750-770	7.87	0.36	4.29	5.7×10^{-4}	102.3
770-790	7.60	0.325	4.45	4.9×10^{-4}	91.2
790-810					

K_r - thermal conductivity of rock matrix
$K\phi$ - in situ thermal conductivity (Sass et al. 1971)
ϕ - porosity
Q - heat flow

TABLE 15. Thermal conductivities and heat flow values for Well CWF-3D.

Depth feet	K_r mcal / cm-sec-C	ϕ	K_ϕ mcal / cm-sec-C	$\Delta T/\Delta z$ C / cm	Q mW / m^2
70-90	6.17	0.35	3.73	9.0×10^{-4}	140.8
90-110	7.64	0.35	4.28	1.8×10^{-4}	32.2
110-130	6.96	0.345	4.06	3.6×10^{-4}	61.3
130-150	5.72	0.34	3.60	8.2×10^{-4}	123.5
150-170	6.24	0.34	3.81	1.08×10^{-3}	172.2
170-190	6.05	0.36	3.63	1.34×10^{-3}	203.5
190-210	5.92	0.365	3.55	1.72×10^{-3}	255.5
210-230	6.61	0.36	3.84	2.34×10^{-3}	376.0
230-250	5.60	0.345	3.52	1.71×10^{-3}	251.8
250-270	5.07	0.365	3.22	1.62×10^{-3}	218.3
270-290	6.33	0.365	3.71	1.44×10^{-3}	223.5
290-310	5.15	0.37	3.23	1.18×10^{-3}	159.5
310-330	5.08	0.355	3.26	1.16×10^{-3}	158.2
330-350	6.32	0.36	3.73	7.2×10^{-4}	112.5
350-370	5.80	0.36	3.53	1.00×10^{-3}	147.7
370-390	5.66	0.35	3.52	9.0×10^{-4}	132.8
390-410	5.44	0.36	3.39	8.0×10^{-4}	114.0
410-430	5.57	0.375	3.37	9.0×10^{-4}	127.2
430-450	5.96	0.375	3.52	7.2×10^{-4}	106.3
450-470	6.99	0.37	3.92	9.0×10^{-4}	147.9
470-490	5.46	0.365	3.37	1.00×10^{-3}	141.0
490-510	6.76	0.365	3.64	9.8×10^{-4}	149.9
510-530	5.91	0.365	3.55	9.0×10^{-4}	134.0
530-550	5.73	0.365	3.48	7.2×10^{-4}	105.1
550-570	5.15	0.355	3.29	8.2×10^{-4}	112.9
570-590	5.05	0.365	3.21	9.8×10^{-4}	132.2
590-610	5.92	0.365	3.55	5.4×10^{-4}	80.4
610-630	4.51	0.37	2.97	5.4×10^{-4}	67.2
630-650	6.25	0.38	3.60	5.4×10^{-4}	81.5
650-670	5.94	0.38	3.48	4.6×10^{-4}	66.8
670-690	8.22	0.38	4.26	3.6×10^{-4}	64.3
690-710	6.95	0.38	3.84	4.4×10^{-4}	71.2
710-730	6.81	0.37	3.85	3.6×10^{-4}	58.2
730-750	6.65	0.365	3.82	3.6×10^{-4}	57.7
750-770	7.28	0.365	4.05	3.6×10^{-4}	61.2
770-790	6.80	0.37	3.85	3.6×10^{-4}	58.2

K_r - thermal conductivity of rock matrix
$K\phi$ - in situ thermal conductivity (Sass et al. 1971)
ϕ - porosity
Q - heat flow

TABLE 16. Thermal conductivities and heat flow values for Well CWF-4D.

Depth feet	K_r mcal / cm-sec-C	ϕ	K_ϕ mcal / cm-sec-C	$\Delta T/\Delta z$ C / cm	Q mW / m^2
70-90	6.53	0.335	3.95	-8.0×10^{-5}	-13.6
90-110	5.91	0.34	3.67	-2.5×10^{-4}	-37.8
110-130	6.35	0.34	3.85	0.0	0.0
130-150	7.53	0.335	4.35	2.5×10^{-4}	44.8
150-170	6.55	0.335	3.96	6.6×10^{-4}	108.7
170-190	5.82	0.335	3.66	7.4×10^{-4}	113.0
190-210	6.50	0.33	3.97	1.15×10^{-3}	191.0
210-230	6.17	0.33	3.83	1.23×10^{-3}	197.1
230-250	6.44	0.34	3.89	1.15×10^{-3}	187.2
250-270	6.94	0.335	4.12	1.07×10^{-3}	184.5
270-290	5.86	0.335	3.68	9.0×10^{-4}	138.9
290-310	6.41	0.335	3.90	9.0×10^{-4}	147.2
310-330	6.71	0.335	4.03	7.4×10^{-4}	124.4
330-350	6.57	0.33	4.00	8.2×10^{-4}	137.2
350-370	6.26	0.325	3.90	8.2×10^{-4}	133.8
370-390	6.32	0.325	3.93	8.2×10^{-4}	134.8
390-410	6.90	0.325	4.17	8.2×10^{-4}	143.1
410-430	6.64	0.320	4.09	7.4×10^{-4}	126.3
430-450	6.09	0.33	3.80	9.0×10^{-4}	143.4
450-470	6.61	0.325	4.05	9.8×10^{-4}	166.7
470-490	6.48	0.33	3.96	8.2×10^{-4}	135.9
490-510	7.06	0.33	4.20	8.2×10^{-4}	144.1
510-530	8.28	0.33	4.67	9.0×10^{-4}	176.2
530-550	6.66	0.335	4.01	6.6×10^{-4}	110.1
550-570	6.20	0.315	3.93	6.6×10^{-4}	107.9
570-590	7.45	0.315	4.46	7.4×10^{-4}	137.7
590-610	6.78	0.31	4.21	9.0×10^{-4}	158.9
610-630	6.96	0.315	4.25	7.4×10^{-4}	131.2
630-650	6.95	0.335	4.12	8.2×10^{-4}	141.4
650-670	7.41	0.315	4.44	7.4×10^{-4}	137.1
670-690	6.64	0.325	4.06	5.7×10^{-4}	97.5
690-710	7.73	0.33	4.46	6.6×10^{-4}	122.4
710-730	7.76	0.33	4.47	4.9×10^{-4}	92.0
730-750	6.90	0.355	3.98	4.9×10^{-4}	81.8
750-770	7.27	0.36	4.08	6.6×10^{-4}	112.0
770-790	8.54	0.355	4.56	4.9×10^{-4}	93.0

K_r - thermal conductivity of rock matrix
$K\phi$ - in situ thermal conductivity (Sass et al. 1971)
ϕ - porosity
Q - heat flow

BIBLIOGRAPHY

Bear, J., and A. Verruijt. 1987. *Modeling Groundwater Flow and Pollution*. Dordrecht: Boston, Massachusetts, 414 p.

Beck, A. E. 1976. An improved method of computing the thermal conductivity of fluid-filled sedimentary rocks. *Geophysics*. 41: 133–144.

Bredehoeft, J. D., and I. S. Papadopulos. 1965. Rates of vertical groundwater movement estimated from the earth's thermal profile. *Water Resources Research*. 1: 325-328.

Burden, R. L., and J. D. Faires. 1989. *Numerical Analysis*. PWS-KENT Publishing Company: Boston, Massachusetts, 729 p.

Currie, I. G. 1974. *Fundamental Mechanics of Fluids*. McGraw-Hill: New York, 441 p.

Deming, D., J. H. Sass, A. H. Lachenbruch, and R. F. DeRito. 1992. Heat flow and subsurface temperature as evidence for basin-scale groundwater flow, North Slope of Alaska. *Geological Society of America Bulletin*. 104: 528–542.

El Paso Water Utilities. 1992. Unpublished pumping schedules 1955–1992. El Paso, Texas.

Freeze, R.A., and J.A. Cherry. 1979. *Groundwater*. Prentice-Hall, Inc: Englewood Cliffs, New Jersey, 604 p.

Keys, W. S., and R. F. Brown. 1978. The use of temperature logs to trace the movement of injected water. *Groundwater*. 16: 32–48.

Mansure, A. J., and M. Reiter. 1979. A vertical groundwater movement correction for heat flow. *J. Geophy. Res.* 84: 3490–3496.

Nickerson, E. L. 1986. *Selected geohydrologic data for the Mesilla Basin, Doña Ana County, New Mexico, and El Paso County, Texas*: U.S. Geological Survey Open-file Report 86-75, Albuquerque, New Mexico.

Nickerson, E. L. 1989. *Aquifer tests in the flood-plain alluvium and Santa Fe Group at the Rio Grande near Cañutillo, El Paso County, Texas*. U.S. Geological Survey Water Resource Investigation Report 89-4011, Albuquerque, New Mexico.

Reiter, M., and H. Hartman. 1971. A new steady-state method for determining thermal conductivity. *J. Geophy. Res.* 76: 7047–7051.

Reiter, M., J. H. Costain, and J. Minier. 1989. Heat flow data and vertical groundwater movement, examples from Southwestern Virginia. *J. Geophy. Res.* 94: 12,423–12,431.

Sass, J. H., A. H. Lachenbruch, and R. J. Munroe. 1971. Thermal conductivity of rocks from measurements on fragments and its application to heat flow determinations. *J. Geophy. Res.* 76: 3391–3401.

Stallman, R. W. 1963. *Computation of groundwater velocity from temperature data*. U.S. Geological Survey Water Supply Paper 1544H, 36–46.

U.S. Geological Survey. 1987. Hydrographs, unpublished. Las Cruces, New Mexico.